L'INSTITUT DE GENIE ELECTRIQUE OTTAWA CARLETON INSTITUTE FOR ELECTRICAL ENGINEERING

ANALYSIS OF TIME-DIVERSITY COMBINING METHODS FOR FREQUENCY-HOPPED SIGNALS

Rolands Ezers and Professor J.S. Wight

Prepared for the Department of Communications
under DSS Contract no. 36001-1-3515

Department of Electronics, Carleton University
Ottawa, Canada

artment of Electronics
Carleton University
Ottawa Canada
K1S 5B6
(613) 788-5754

Département de génie électrique/
Department of Electrical Engineering
Université d'Ottawa/
University of Ottawa
Ottawa Canada
K1N 6N5
(613) 564-8213

Department of Systems and
Computer Engineering
Carleton University
Ottawa Canada
K1S 5B6
(613) 788-5740

L'INSTITUT DE GENIE ELECTRIQUE OTTAWA CARLETON INSTITUTE FOR ELECTRICAL ENGINEERING

ANALYSIS OF TIME-DIVERSITY COMBINING METHODS FOR FREQUENCY-HOPPED SIGNALS

Rolands Ezers and Professor J.S. Wight

Prepared for the Department of Communications
under DSS Contract no. 36001-1-3515

Department of Electronics, Carleton University
Ottawa, Canada

Department of Electronics
Carleton University
Ottawa Canada
K1S 5B6
(613) 788-5754

Département de génie électrique/
Department of Electrical Engineering
Université d'Ottawa/
University of Ottawa
Ottawa Canada
K1N 6N5
(613) 564-8213

Department of Systems and
Computer Engineering
Carleton University
Ottawa Canada
K1S 5B6
(613) 788-5740

ANALYSIS OF TIME-DIVERSITY COMBINING METHODS FOR FREQUENCY-HOPPED SIGNALS

Rolands Ezers and Professor J.S. Wight

Prepared for the Department of Communications
under DSS Contract no. 36001-1-3515

Department of Electronics, Carleton University
Ottawa, Canada

April 1992

DOE-92-09

Abstract

This report discusses fast-frequency-hopped (FFH) noncoherent-frequency-shift-keyed (NCFSK) communication systems with time diversity and diversity combining. A literature review of diversity-combining techniques is provided. An analytical method has been developed for one of the techniques, linear combining. The method combines circularly symmetric function theory, Fourier-Bessel series, and Fourier series. With this method, the bit-error probability for the demodulation of FFH NCFSK systems with time diversity and linear diversity combining and the probability of detection and probability of false alarm for uplink coarse-time synchronization of a FFH NCFSK satellite-communication system with time diversity and linear diversity combining have been computed in broad-band noise and multiple-tone jamming. Where possible, the results obtained with this method were compared to other reported results, and the two results agreed well. A novel analytical result was derived for computing the bit-error probability for the demodulation of FFH NCFSK systems with time diversity and 4-2- or 2-1-moment-method diversity combining in independent Rayleigh fading.

For demodulation, linear diversity combining is an excellent method in broad-band noise. In severe multiple-tone jamming, linear diversity combining is good. In weak multiple-tone jamming, linear diversity combining is not a good method because it is susceptible to Houston-sense multiple-tone jamming with a small jamming fraction. In independent Rayleigh fading, square-law combining is the best method for the particular situation which was considered.

For uplink coarse-time synchronization, time diversity and linear diversity combining could be used to improve performance.

Contents

List of Figures

List of Tables

Chapter 1

Introduction

1.1 Objectives

Fast-frequency-hopped (FFH) noncoherent-frequency-shift-keyed (NCFSK) communication systems have inherent time diversity which can be used to improve anti-jam capabilities for demodulation. Time diversity is introduced at the transmitter by fast hopping and is removed at the receiver by an operation called diversity combining. There are many methods of diversity combining. Considerable work has been done in obtaining measures of performance for these methods in various interference and fading environments. However, because of the complexity of the problem, most work has involved special cases, simplifications, or computer simulation, and many aspects of the problem have not been considered.

Time diversity and diversity combining can also be used to improve the anti-jam performance for uplink coarse-time synchronization and uplink fine-time synchronization of a FFH NCFSK satellite-communication system. The diversity-combining methods are similar to those used for demodulation. Little work has been done in obtaining measures of performance for coarse-time or fine-time synchronization for any of the diversity-combining methods.

Analytical techniques would provide insight into some aspects of the demodulation and synchronization problems; however, such techniques are quite difficult to derive. In this report, the objective is to develop analytical techniques for obtaining performance measures for FFH NCFSK systems. The analytical techniques can then be used to gain insight into the demodulation performance of FFH NCFSK systems and into the uplink-coarse-time-synchronization performance of a FFH NCFSK satellite-communication system.

1.2 Scope

In this report, a novel analytical technique is developed which can provide the general solution for one diversity-combining technique – linear diversity combining. Measures of performance are obtained in broad-band noise, multiple-tone jamming, and Rayleigh fading for demodulation in FFH NCFSK systems. Measures of performance are also obtained in broad-band noise, and multiple-tone jamming for uplink coarse-time synchronization in a FFH NCFSK satellite-communication system.

Also, a novel analytical technique is developed for obtaining performance of a special case of 4-2- or 2-1-moment-method diversity combining in Rayleigh fading for demodulation of FFH NCFSK systems.

1.3 Outline

Chapter 2 presents a background in modulation and demodulation of FFH NCFSK systems with time diversity and diversity combining and in uplink coarse-time synchronization of a FFH NCFSK satellite-communication system. Chapter 3 presents the analysis method for linear combining. Chapter 4 presents performance results for demodulation in FFH NCFSK systems with time diversity and diversity combining. Chapter 5 presents performance results for uplink coarse-time synchronization in a FFH NCFSK satellite-communication system. Chapter 6 presents conclusions.

Chapter 2

Background

2.1 Introduction

This chapter presents a background in the modulation and demodulation of FFH NCFSK communications systems with time diversity and diversity combining. Frequency-hopped communication is achieved by varying the carrier frequency of the transmitted signal pseudorandomly over a wide bandwidth. The receiver has knowledge of the hopping sequence and knows in which frequency channel the transmitted signal is located at a given time. The receiver can then demodulate the signal. Demodulation is performed assuming perfect time synchronization and frequency synchronization between the transmitter and the receiver. A coarse-time-synchronization algorithm is discussed towards the end of this chapter for the uplink of a FFH NCFSK satellite-communication system.

2.2 Modulation and Demodulation for FFH NCFSK Systems

The transmitter considered in this report is shown in Fig. 2.1. Binary data is passed through an error-correction encoder. The coded bits are then converted to M-ary symbols with period, T_s. The M-ary symbols are applied to a frequency synthesizer where the output signal is a tone at frequency, f_m, having one of M possible frequencies. For the ith hop period, the symbols are mixed with a frequency tone, f_{hi}, generated by a frequency synthesizer driven by a pseudonoise-code generator. The tone, f_{hi}, has a hop duration, $T_h = T_m/L$. The hop rate for the system is fixed. The integer, L, is the number of hops per symbol and is termed the diversity level. If $L \geq 1$, the system is called fast

frequency hopped; in this report, only fast-frequency-hopped systems are considered. The transmitted waveform consists of a series of tones at frequency, $f_{hi} + f_m$, of duration, T_h.

As shown in Fig. 2.2, the received signal is mixed with the output of a local frequency synthesizer driven by the same pseudorandom code used at the transmitter. The output of the mixer is then a tone, f_m, of duration, T_h. This tone is passed through a bank of M matched filters with envelope detectors which is shown in Fig. 2.3. Each filter is matched to one of the M tones, f_m, and uses noncoherent detection. A matched filter with envelope detector is shown in Fig. 2.4. The outputs are the samples, z_{mi}, for $m = 1, ..., M$, and $i = 1, ..., L$. The subscript, m, denotes the frequency bin, and the subscript, i, denotes the hop period. The diversity combiner forms the decision statistics, v_m, based upon the L samples, z_{mi}, using one of many diversity-combining techniques. A decision is then made as to which symbol was sent based on these M statistics. The M-ary symbols are then converted to binary and passed to the error-correction decoder. Finally, the binary data is received from the decoder.

2.3 Optimum Receiver

The optimum receiver for a FFH NCFSK system can be found using Karhunen-Loève expansions and Bayes' criterion [1]. For additive white Gaussian noise (AWGN), this results in a receiver consisting of a bank of matched filters with envelope detectors followed by a diversity combiner. The optimum method of diversity combining involves calculating the *a posteriori* probability for each hypothesis [1]. Therefore, the decision statistic is

$$\Lambda_m = \text{Probability(tone } m \text{ sent} \mid z_{mi},\ i = 1, ..., L,\ m = 1, ..., M). \tag{2.1}$$

The largest Λ_m indicates the most probable tone that was sent.

For M-ary communication in AWGN, the optimum statistic can be derived from (2.1) and is given by

$$v_m = \sum_{i=1}^{L} \ln(I_0(\frac{z_{mi}s_i}{\sigma^2})) \tag{2.2}$$

where s_i is the rms signal-tone amplitude on the ith hop period, $\sigma^2 = N_0/2T_h$, $N_0/2$ is the two-sided noise power-spectral density, and $I_0()$ is the zeroth-order modified-Bessel function. The largest v_m indicates the transmitted tone. This result was first derived for the binary case in [2]. The combining method of (2.2) is often called "optimum combining" [2],[4], but it requires knowledge of s_i and σ. Since these are not known *a priori*, they

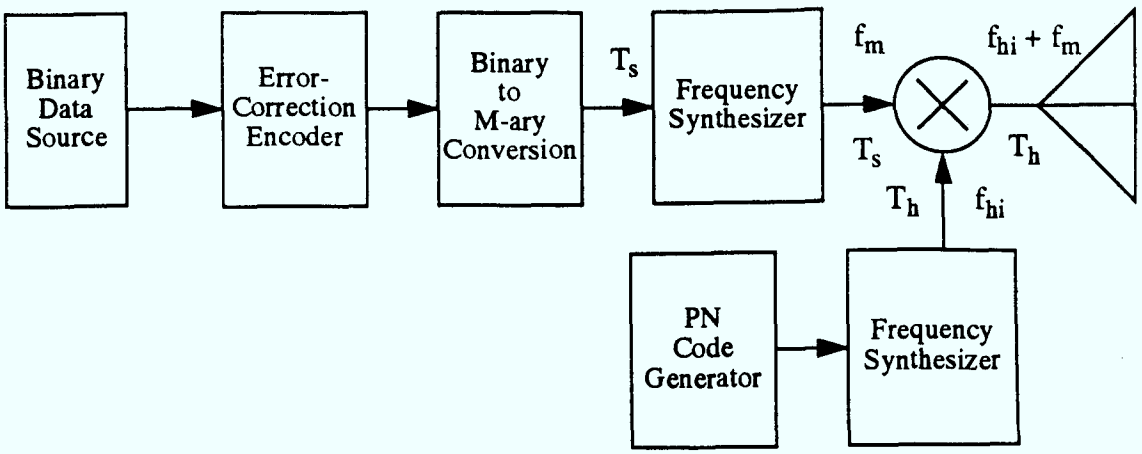

Figure 2.1: A frequency-hopped system transmitter.

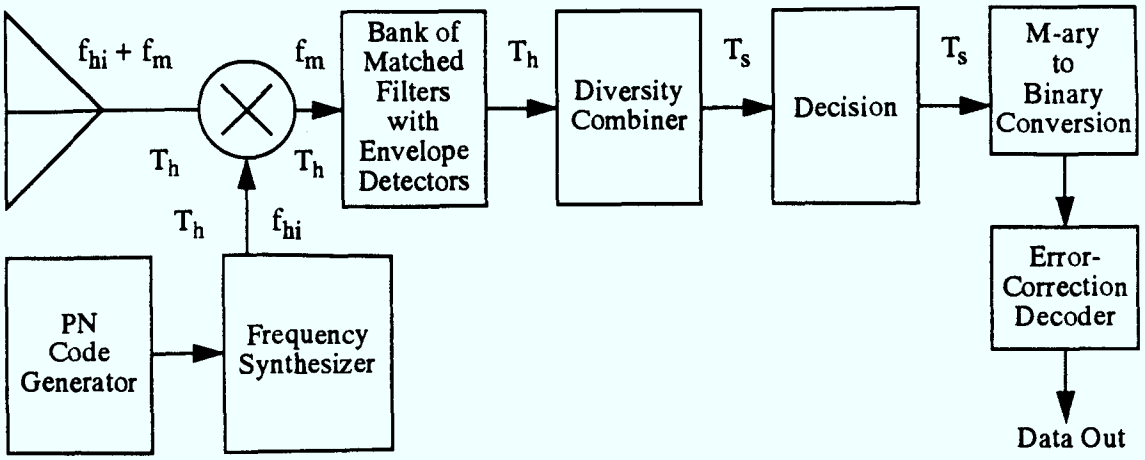

Figure 2.2: A frequency-hopped system receiver.

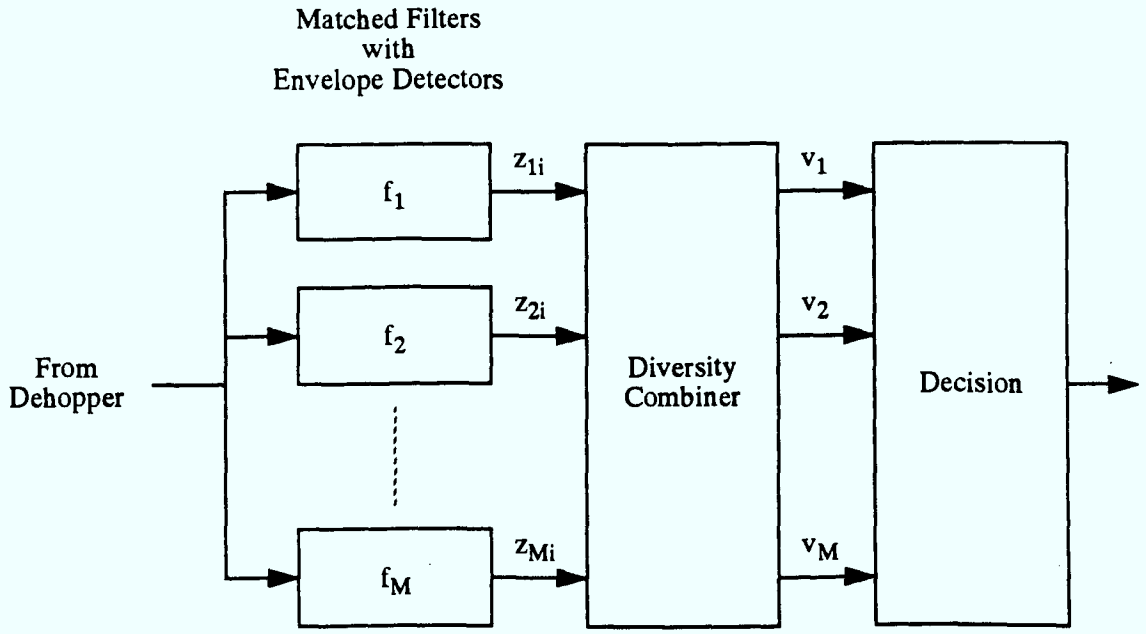

Figure 2.3: A bank of matched filters with envelope detectors.

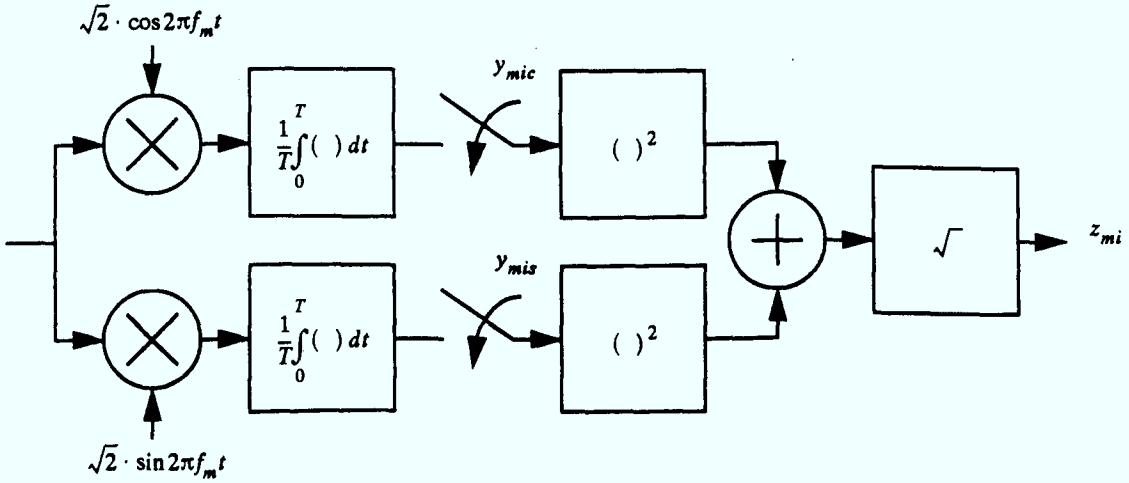

Figure 2.4: A matched filter with envelope detector.

must somehow be estimated, and therefore, it is not practical to use this method in an actual system. It is desirable to have a decision statistic which does not require knowledge of s_i or σ. Below, many other diversity-combining methods are presented.

2.4 Diversity-Combining Methods

2.4.1 Selection Diversity Combining

This combining technique, sometimes called switched diversity combining, picks the largest z_{mi} over the L hop periods as the decision statistic. Thus, [5]

$$v_m = \max_i(z_{mi}). \tag{2.3}$$

The largest v_m indicates the transmitted tone.

2.4.2 Linear Diversity Combining

If $z_{mi}s_i/\sigma^2 >> 1$, the statistic of (2.2) can be approximated using $I_0(x) \approx \exp(x)/\sqrt{2\pi x}$ [3]. Taking the logarithm of both sides, $\ln(I_0(x)) \approx x - (0.5\ln(2\pi x))$. For $x >> 1$, $x >> 0.5\ln(2\pi x)$. Now, the statistic is [2],[4],[6]-[9]

$$\sum_{i=1}^{L} \ln(I_0(\frac{z_{mi}s_i}{\sigma^2})) \approx \sum_{i=1}^{L} \frac{z_{mi}s_i}{\sigma^2}. \tag{2.4}$$

Assuming that s_i and σ do not change from hop to hop, a decision statistic is

$$v_m = \sum_{i=1}^{L} z_{mi}. \tag{2.5}$$

The largest v_m indicates the transmitted tone. This combining method is called "linear combining" and should also have near-optimal performance in AWGN.

2.4.3 Square-Law Diversity Combining

If $z_{mi}s_i/\sigma^2 << 1$, the statistic of (2.2) can be approximated using $I_0(x) \approx 1 + (x^2/4)$ and $\ln(1+x) \approx x$ [3]. This results in [2],[4],[5],[10]-[14]

$$\sum_{i=1}^{L} \ln(I_0(\frac{z_{mi}s_i}{\sigma^2})) \approx \sum_{i=1}^{L} \frac{z_{mi}^2 s_i^2}{4\sigma^4}. \tag{2.6}$$

Assuming that s_i and σ do not change from hop to hop, the decision statistic can be chosen as

$$v_m = \sum_{i=1}^{L} z_{mi}^2. \tag{2.7}$$

The largest v_m indicates the transmitted tone. This combining method is called "square-law combining" and should have near-optimal performance in AWGN.

2.4.4 Hard-Decision-Majority-Vote Diversity Combining

Hard-decision-majority-vote (HDMV) diversity combining performs a hard decision on each hop. This means that [9],[15],[16]

$$f_{hdmv}(z_{mi}) = \begin{cases} 1, & z_{mi} \geq z_{ki} \text{ for all k} \\ 0, & \text{otherwise} \end{cases} . \tag{2.8}$$

Then, the decision statistic is

$$v_m = \sum_{i=1}^{L} f_{hdmv}(z_{mi}). \tag{2.9}$$

The largest v_m indicates the transmitted tone.

2.4.5 Ratio-Statistic-Envelope Diversity Combining

Ratio-statistic-envelope diversity combining normalizes samples on each hop by the largest of the samples on that hop and then sums the normalized samples. Thus, the decision statistic is [4],[13],[17]

$$v_m = \sum_{i=1}^{L} \frac{z_{mi}}{\max_m(z_{mi})}. \tag{2.10}$$

The largest v_m indicates the transmitted tone.

2.4.6 Self-Normalized-Envelope Diversity Combining

Self-normalized-envelope (SNE) diversity combining, sometimes called normalized-envelope detection (NED), normalizes samples on each hop by the sum of the samples on that hop and then sums the normalized samples. Thus, the decision statistic is [9],[13],[16],[18]-[21]

$$v_m = \sum_{i=1}^{L} \frac{z_{mi}}{\sum_{m=1}^{M} z_{mi}}. \tag{2.11}$$

The largest v_m indicates the transmitted tone.

2.4.7 Ratio-Statistic-Square-Law Diversity Combining

Ratio-statistic-square-law diversity combining normalizes the squares of the samples on each hop by the square of the largest sample on that hop and then sums the normalized

samples. Thus, the decision statistic is [13]

$$v_m = \sum_{i=1}^{L} \frac{z_{mi}^2}{\max_m(z_{mi}^2)}. \tag{2.12}$$

The largest v_m indicates the transmitted tone.

2.4.8 Self-Normalized-Square-Law Diversity Combining

Self-normalized-square-law diversity combining normalizes the squares of the samples on each hop by the sum of the squares of the samples on that hop and then sums the normalized samples. Thus, the decision statistic is [13],[22]

$$v_m = \sum_{i=1}^{L} \frac{z_{mi}^2}{\sum_{m=1}^{M} z_{mi}^2}. \tag{2.13}$$

The largest v_m indicates the transmitted tone.

2.4.9 Clipped-Linear Diversity Combining

Clipped-linear diversity combining clips the samples at a prescribed level above the desired-signal level and then sums the clipped samples. This means that [7]

$$f_{cl}(z_{mi}) = \begin{cases} C, & \text{for } z_{mi} \geq C \\ z_{mi}, & \text{otherwise} \end{cases}. \tag{2.14}$$

Then,

$$v_m = \sum_{i=1}^{L} f_{cl}(z_{mi}). \tag{2.15}$$

The largest v_m indicates the transmitted tone. It requires side information to set the threshold, C.

2.4.10 Clipped-Square-Law Diversity Combining

Clipped-square-law diversity combining clips the squares of the samples at a prescribed level above the desired-signal level and then sums the clipped samples. This means that [13],[14]

$$f_{csl}(z_{mi}) = \begin{cases} C, & \text{for } z_{mi}^2 \geq C \\ z_{mi}^2, & \text{otherwise} \end{cases}. \tag{2.16}$$

Then,

$$v_m = \sum_{i=1}^{L} f_{csl}(z_{mi}). \tag{2.17}$$

The largest v_m indicates the transmitted tone. It requires side information to set the threshold, C.

2.4.11 Ratio-Threshold-Square-Law Diversity Combining

The ratio-threshold technique orders the input data from smallest to largest. It then takes the ratio of the two largest samples on each hop and assigns on each hop a quality factor, q_i, of 1 (good) if the ratio is greater than a threshold and assigns a factor of 0 (bad) if the ratio is less than the threshold. The threshold is chosen to be greater than 1. The decision statistic is formed by [23]

$$v_m = \sum_{i=1}^{L} q_i z_{mi}^2. \tag{2.18}$$

The largest v_m indicates the transmitted tone. If all $q_i = 0$ for $i = 1, ..., L$, then a decision is based on the z_{mi} with the largest sample ratio.

2.4.12 Ratio-Threshold-Majority-Logic Diversity Combining

The ratio-threshold-majority-logic method assigns the same quality factor to each hop period as the ratio-threshold-square-law method. Then, a hard decision is performed on each hop. This means that [23],[24]

$$f_{rtml}(z_{mi}) = \begin{cases} 1, & z_{mi} \geq z_{ki} \text{ for all k} \\ 0, & \text{otherwise} \end{cases}. \tag{2.19}$$

The decision statistic is formed by

$$v_m = \sum_{i=1}^{L} q_i f_{rtml}(z_{mi}). \tag{2.20}$$

The largest v_m indicates the transmitted tone. If all $q_i = 0$ for $i = 1, ..., L$, then a decision is based on the z_{mi} with the largest sample ratio.

2.4.13 4-2-Moment-Method Diversity Combining

The 4-2-moment-method diversity combining forms a decision statistic, [9],[19]

$$v_m = 2(\frac{1}{L}\sum_{i=1}^{L} z_{mi}^2)^2 - (\frac{1}{L}\sum_{i=1}^{L} z_{mi}^4). \tag{2.21}$$

The largest v_m indicates the transmitted tone. This method attempts to subtract the interference power from the samples.

2.4.14 2-1-Moment-Method Diversity Combining

The 2-1-moment-method diversity combining forms a decision statistic, [9],[19],[20]

$$v_m = 2(\frac{1}{L}\sum_{i=1}^{L} z_{mi})^2 - (\frac{1}{L}\sum_{i=1}^{L} z_{mi}^2). \tag{2.22}$$

The largest v_m indicates the transmitted tone. This method also attempts to subtract the interference power from the samples.

2.4.15 1-1/2-Moment-Method Diversity Combining

The 1-1/2-moment-method diversity combining forms a decision statistic, [9]

$$v_m = 2(\frac{1}{L}\sum_{i=1}^{L} \sqrt{z_{mi}})^2 - (\frac{1}{L}\sum_{i=1}^{L} z_{mi}). \tag{2.23}$$

The largest v_m indicates the transmitted tone. This method also attempts to subtract the interference power from the samples.

2.4.16 Order-Statistic Diversity Combining

The use of order statistics (OS) for diversity combining requires the sorting of the L values in each bin so that

$$z_{mi_1} \leq z_{mi_2} \leq \cdots \leq z_{mi_{L-1}} \leq z_{mi_L}, \quad m = 1, 2, \cdots, M \tag{2.24}$$

where z_{mi_1} is the smallest OS of the mth bin, and z_{mi_L} is the largest OS of the mth bin. For a previously specified value of l, the decision statistic is chosen as [9],[25]-[27]

$$v_m = z_{mi_l}. \tag{2.25}$$

The largest v_m indicates the transmitted tone.

2.4.17 Weighted-Order-Statistic Diversity Combining

Order-statistic processing is done first by (2.24) in order to rank z_{mi}. Then, the ranked values are summed by [8],[27]

$$v_m = \sum_{l=1}^{L} w_{mi_l} z_{mi_l} \tag{2.26}$$

where w_{mi_l} are weights. The largest v_m indicates the transmitted tone.

2.4.18 Order-Statistic-Self-Normalized-Envelope Diversity Combining

The order-statistic and self-normalized-envelope methods can be combined to form OSSNE combining. Order-statistic processing is done first by (2.24) in order to rank the z_{mi}. Then, the ranked values are normalized to

$$\widehat{z_{mi_l}} = \frac{z_{mi_l}}{\sum_{m=1}^{M} z_{mi_l}}. \tag{2.27}$$

The decision statistic is formed by [26],[27]

$$v_m = \sum_{l=1}^{L} \widehat{z_{mi_l}}. \tag{2.28}$$

The largest v_m indicates the transmitted tone.

2.4.19 Order-Statistic-Hard-Decision-Majority-Vote Diversity Combining

The order-statistic and hard-decision-majority-vote methods can be combined to form OSHDMV combining. Order-statistic processing is done first by (2.24) in order to rank z_{mi}. Then, on each hop period, a hard decision is made such that

$$f_{oshdmv}(z_{mi_l}) = \begin{cases} 1, & z_{mi_l} \geq z_{ki_l} \text{ for all k} \\ 0, & \text{otherwise} \end{cases}. \tag{2.29}$$

Then, the decision statistic is

$$v_m = \sum_{i=1}^{L} f_{oshdmv}(z_{mi_l}). \tag{2.30}$$

The largest v_m indicates the transmitted tone.

2.4.20 Weighted-Order-Statistic-Self-Normalized-Envelope Diversity Combining

This method forms a weighted sum of the modified values in the OSSNE method. The decision statistic is [27]

$$v_m = \sum_{l=1}^{L} w_{mi_l} \widehat{z_{mi_l}} \tag{2.31}$$

where w_{mi_l} are the weights. The largest v_m is chosen as the transmitted symbol.

2.4.21 Recursive-Excision Diversity Combining

The average of the L values in each bin is computed as [27]

$$v_m = \frac{1}{L}\sum_{i=1}^{L} z_{mi}. \tag{2.32}$$

The ratios,

$$q_{mi} = z_{mi}/v_m, \tag{2.33}$$

are calculated on each iteration. If any of the q_{mi} exceed the threshold, C, the corresponding z_{mi} is deleted from the L-bin values, and L is decremented for that bin only. The calculations (2.32) and (2.33) are iterated until $q_{mi} \leq C$ for all remaining bin values. The decision statistics are then the final averages from (2.32). The largest v_m is chosen as the transmitted symbol.

2.5 Literature Review

This section provides a literature review of previous work in obtaining performance measures for the demodulation of FFH NCFSK systems with time diversity and diversity combining. Previous work, which is summarized in Table 2.1 and Table 2.2, presents results from theoretical analysis, computer simulation, or experimental analysis of various systems in different interference and fading environments. Prior to reviewing the literature, some terminology pertaining to the types of interference and fading must be introduced. In a broad-band-noise environment, the system is subjected to AWGN across its entire bandwidth. In a partial-band-noise environment, the system is subjected to AWGN across part of its bandwidth. In a tone-jamming environment, the system is subjected to multiple-tone interference. In an independent-Rayleigh-fading environment, the fluctuating signal amplitude has a Rayleigh probability distribution. In an independent-Rician-fading environment, the fluctuating signal amplitude has a Rician probability distribution. In a correlated-fading environment, fluctuations in signal amplitude are correlated across hop periods.

Optimum diversity combining is discussed in [2] and [4]. In [2], the probability of error for a FFH binary NCFSK system in broad-band noise is presented. Results are generated by computer simulation for levels of diversity ranging from $L = 1$ to $L = 10$. In [4], the probability of error for a FFH 8-ary NCFSK system is presented for two cases: partial-band noise with broad-band noise, and tone jamming with broad-band noise. Results are generated by computer simulation for $L = 4$.

Combining Method	Ref.	Analysis	Interference
optimum	[2]	simulation	broad-band noise
	[4]	simulation	tone jamming, partial-band noise
selection	[5]	exact	Rayleigh fading, broad-band noise
linear	[2]	simulation	broad-band noise
	[6]	bounds	partial-band noise, tone jamming
	[7]	exact	partial-band noise
	[8]	simulation	partial-band noise
	[4]	simulation	tone jamming, Rayleigh fading, partial-band noise
	[9]	simulation	broad-band noise
square-law	[5]	exact	Rayleigh fading, broad-band noise
	[10]	exact	Rayleigh fading, broad-band noise
	[11]	exact	Rician fading, broad-band noise
	[12]	exact	Rician fading, broad-band noise
	[2]	simulation	broad-band noise
	[13]	assumptions	partial-band noise
	[14]	bounds	partial-band noise
	[4]	simulation	tone jamming, Rayleigh fading, broad-band noise
hard-decision-majority-vote	[15]	exact	partial-band noise, tone jamming
	[16]	experiment	partial-band noise, tone jamming
	[9]	simulation	broad-band noise, tone jamming
ratio-statistic-envelope	[13]	simulation	partial-band noise
	[17]	exact	partial-band noise
	[4]	simulation	partial-band noise, tone jamming, Rayleigh fading

Table 2.1: Literature Review of Diversity-Combining Techniques

Combining Method	Ref.	Analysis	Interference
self-normalized-envelope	[13]	simulation	partial-band noise, tone jamming
	[18]	assumptions	tone jamming
	[16]	experiment	partial-band noise, tone jamming
	[9]	simulation	broad-band noise, tone jamming
	[19]	simulation	broad-band noise, tone jamming
	[20]	simulation	broad-band noise, tone jamming
	[21]	exact	Rician fading, partial-band noise
ratio-statistic-square-law	[13]	simulation	partial-band noise
self-normalized-square law	[13]	simulation	partial-band noise, tone jamming
	[22]	exact	partial-band noise
clipped-linear	[7]	exact	partial-band noise, Rician fading
clipped-square-law	[13]	simulation	partial-band noise
	[14]	exact	partial-band noise
ratio-threshold-square-law	[23]	exact	Rician fading, partial-band noise
ratio-threshold-majority-logic	[23]	exact	Rician fading, partial-band noise
	[24]	exact	tone jamming
4-2-moment-method	[9]	simulation	partial-band noise, tone jamming
2-1-moment-method	[9]	simulation	partial-band noise, tone jamming
	[19]	simulation	partial-band noise, tone jamming
	[20]	simulation	partial-band noise, tone jamming
1-1/2-moment-method	[9]	simulation	partial-band noise, tone jamming
order-statistic	[25]	exact	partial-band noise
	[9]	simulation	broad-band noise, tone jamming
	[26]	simulation	broad-band noise, tone jamming
	[27]	simulation	broad-band noise, tone jamming
weighted-order-statistic	[8]	simulation	partial-band noise
	[27]	simulation	broad-band noise, tone jamming
OSSNE	[26]	simulation	broad-band noise, tone jamming
	[27]	simulation	broad-band noise, tone jamming
WOSSNE	[27]	simulation	broad-band noise, tone jamming
recursive-excision	[27]	simulation	broad-band noise, tone jamming

Table 2.2: Literature Review of Diversity-Combining Techniques continued

Selection diversity combining is discussed in [5]. The probability of error for a binary NCFSK system in broad-band noise with independent Rayleigh fading is derived. Exact analysis is used for arbitrary level of diversity. Results are shown for $L = 2, ..., 10$.

Linear diversity combining is discussed in [2], [4], and [6]-[9]. In [2], the probability of error for a FFH binary NCFSK system in broad-band noise is presented. Results are generated by computer simulation for $L = 1, ..., 10$. In [6], the probability of error for a FFH M-ary NCFSK system is presented for three cases: broad-band noise, partial-band noise, and tone jamming. Each case is treated separately. The analysis makes simplifying assumptions and uses bounds. Side information concerning the hops that are jammed is assumed to be available. Results are presented for $M = 16$ and optimum level of diversity. In [7], the probability of bit error is calculated for a FFH M-ary NCFSK system in partial-band noise jamming using an analytical method based on repeated convolutions which is only practical for small levels of diversity. Results are shown for $L = 3$. In [8], the probability of error for a FFH M-ary NCFSK system is presented for partial-band noise with broad-band noise. Results are generated by computer simulation for $L = 1, 3$ and $M = 4, 8, 16$. In [4], the probability of error for a FFH 8-ary NCFSK system is presented for two cases: tone jamming with broad-band noise, and broad-band noise with independent Rayleigh fading. Results are generated by computer simulation for tone jamming with $L = 2$ and for Rayleigh fading with $L = 8$. In [9], the probability of error for a FFH 8-ary NCFSK system is presented for two cases: broad-band noise, and tone jamming with broad-band noise. Results are generated by computer simulation for $L = 1, ..., 32$.

Square-law diversity combining is discussed in [2], [4], [5], and [10]-[14]. In [5], the probability of error for a binary NCFSK system is presented for three cases: independent Rayleigh fading with broad-band noise, correlated Rayleigh fading with broad-band noise and independent Rayleigh fading with correlated noise. Exact analysis is used. Results are presented for the above three cases with $L = 1, ..., 20$, $L = 2$, and $L = 2, ..., 10$, respectively. In [10], the probability of error for a M-ary NCFSK system is presented for independent Rayleigh fading with broad-band noise. Exact analysis is used. Results are presented for $M = 2$ with $L = 1, ..., 20$, for $M = 4$ with $L = 1, ..., 10$, and for $M = 8$ with $L = 1, ..., 5$. In [11], the probability of error for a M-ary NCFSK system is presented for independent Rayleigh and Rician fading with broad-band noise. Exact analysis is used for arbitrary M and L. Results are presented for $M = 2$ with $L = 1, ..., 19$. In [12], the probability of error for a binary NCFSK system is presented for correlated Rayleigh and Rician fading with broad-band noise. Exact analysis is used. Results are presented

for $M = 2$ with $L = 1, ..., 15$. In [2], the probability of error for a FFH binary NCFSK system in broad-band noise is presented. Results are generated by computer simulation for $L = 1, ..., 10$. In [13], the probability of error for a FFH M-ary NCFSK system is presented for two cases: broad-band noise, and partial-band noise. For broad-band noise, exact analysis is used for arbitrary M and L. Results are presented for $M = 8$ with $L = 1, ..., 64$. For partial-band noise, the analysis assumes no broad-band noise. Results are presented for $M = 8$ with $L = 1, ..., 8$. In [14], the probability of error for a FFH binary NCFSK system is presented for partial-band noise with broad-band noise. Exact analysis is performed for arbitrary L. Results are presented for $L = 1, ..., 6$. Results from exact analysis are compared to results calculated by using bounds. In [4], the probability of error for a FFH 8-ary NCFSK system is presented for two cases: tone jamming with broad-band noise, and broad-band noise with Rayleigh fading. Results are generated by computer simulation for $L = 2, 4$.

Hard-decision-majority-vote diversity combining is discussed in [9], [15], and [16]. In [15], the probability of error for a FFH M-ary NCFSK system is presented for two cases: tone jamming with broad-band noise, and partial-band noise with broad-band noise. Exact analysis is presented for arbitrary M and L. Results are presented for $M = 2, 8$ and $L = 1, ..., 9$. In [16], the probability of error for a FFH 8-ary NCFSK system is measured for two cases: tone jamming with broad-band noise, and partial-band noise with broad-band noise. Experimental data is presented for $L = 1, ..., 32$. In [9], the probability of error for a FFH 8-ary NCFSK system is presented for two cases: tone jamming with broad-band noise, and broad-band noise. Results are generated by computer simulation for $L = 1, ..., 32$.

Ratio-statistic-envelope diversity combining is discussed in [4], [13], and [17]. In [13], the probability of error for a FFH 8-ary NCFSK system is presented for two cases: broad-band noise, and partial-band noise. Results are generated by computer simulation for $L = 1, ..., 6$. In [17], the probability of error for a FFH binary NCFSK system is presented for partial-band noise with broad-band noise. Exact analysis is presented for arbitrary L. Results are presented for $L = 1, ..., 5$. In [4], the probability of error for a FFH 8-ary NCFSK system is presented for three cases: partial-band noise with broad-band noise, tone jamming with broad-band noise, and broad-band noise with Rayleigh fading. Results are generated by computer simulation for $L = 4$.

Self-normalized-envelope diversity combining is discussed in [9], [13], [16], and [18]-[21]. In [13], the probability of error for a FFH 8-ary NCFSK system is presented for three

cases: broad-band noise, partial-band noise, and tone jamming. Results are generated by computer simulation for $L = 1, ..., 6$. In [18], the probability of error for a FFH binary NCFSK system is presented for tone jamming. Approximate results are derived for arbitrary L since broad-band noise is not considered. In [16], the probability of error for a FFH 8-ary NCFSK system is measured for two cases: tone jamming with broad-band noise, and partial-band noise with broad-band noise. Experimental data is presented for $L = 1, ..., 32$. In [19], the probability of error for a FFH 8-ary NCFSK system is presented for two cases: tone jamming with broad-band noise, and broad-band noise. Results are generated by computer simulation for $L = 1, ..., 32$. In [20], the probability of error for a FFH 8-ary NCFSK system is presented for two cases: tone jamming with broad-band noise, and broad-band noise. Results are generated by computer simulation for $L = 1, ..., 28$. In [9], the probability of error for a FFH 8-ary NCFSK system is presented for two cases: tone jamming with broad-band noise, and broad-band noise. Results are generated by computer simulation for $L = 1, ..., 28$. In [21], the probability of error for a FFH binary NCFSK system is presented for partial-band noise with broad-band noise and independent Rician fading. Exact analysis is presented for arbitrary L. Results are presented for $L = 1, ..., 4$.

Ratio-statistic-square-law diversity combining is discussed in [13]. The probability of error for a FFH 8-ary NCFSK system is presented for two cases: broad-band noise, and partial-band noise. Results are generated by computer simulation for $L = 1, ..., 6$.

Self-normalized-square-law diversity combining is discussed in [13] and [22]. In [13], the probability of error for a FFH 8-ary NCFSK system is presented for three cases: broad-band noise, partial-band noise, and tone jamming. Results are generated by computer simulation for $L = 1, ..., 6$. In [22], the probability of error for a FFH binary NCFSK system is presented for partial-band noise with broad-band noise. Exact analysis is presented for arbitrary L. Results are presented for $L = 1, ..., 4$.

Clipped-linear diversity combining is discussed in [7]. The probability of error for a FFH M-ary NCFSK system is presented for partial-band noise with broad-band noise. Exact analysis is presented for arbitrary L and M. Results are presented for $M = 32$ and $L = 3, 5$.

Clipped-square-law diversity combining is discussed in [13] and [14]. In [13], the probability of error for a FFH 8-ary NCFSK system is presented for three cases: broad-band noise, partial-band noise, and tone jamming. Results are generated by computer simulation for $L = 1, ..., 6$. In [14], the probability of error for a FFH binary NCFSK system is

presented for partial-band noise with broad-band noise. Exact analysis is presented for arbitrary L. Results are presented for $L = 1, 2$.

Ratio-threshold-square-law diversity combining is discussed in [23]. The probability of error for a FFH binary NCFSK system is presented for three cases: partial-band noise with broad-band noise, independent Rayleigh fading with broad-band noise, and independent Rician fading with broad-band noise. Exact analysis is presented for arbitrary L. Results are presented for $L = 1, ..., 5$.

Ratio-threshold-majority-logic diversity combining is discussed in [23] and [24]. In [23], the probability of error for a FFH binary NCFSK system is presented for three cases: partial-band noise with broad-band noise, independent Rayleigh fading with broad-band noise, and independent Rician fading with broad-band noise. Exact analysis is presented for arbitrary L. Results are presented for $L = 1, ..., 5$. In [24], the probability of error for a FFH binary NCFSK system is derived for partial-band noise with broad-band noise, and and tone jamming with broad-band noise. Results are presented for $L = 4$ and $M = 2, 8$.

The 4-2-moment-method diversity combining is discussed in [9] and [19]. In [19], the probability of error for a FFH 8-ary NCFSK system is presented for two cases: partial-band noise with broad-band noise, and tone jamming with broad-band noise. Results are generated by computer simulation for $L = 1, ..., 32$. In [9], the probability of error for a FFH 8-ary NCFSK system is presented for two cases: partial-band noise with broad-band noise, and tone jamming with broad-band noise. Results are generated by computer simulation for $L = 1, ..., 32$.

The 2-1-moment-method diversity combining is discussed in [9], [19], and [20]. In [19], the probability of error for a FFH 8-ary NCFSK system is presented for two cases: partial-band noise with broad-band noise, and tone jamming with broad-band noise. Results are generated by computer simulation for $L = 1, ..., 32$. In [9], the probability of error for a FFH 8-ary NCFSK system is presented for two cases: partial-band noise with broad-band noise, and tone jamming with broad-band noise. Results are generated by computer simulation for $L = 1, ..., 32$. In [20], the probability of error for a FFH 8-ary NCFSK system is presented for two cases: partial-band noise with broad-band noise, and tone jamming with broad-band noise. Results are generated by computer simulation for $L = 1, ..., 28$.

The 1-1/2-moment-method diversity combining is discussed in [9]. The probability of error for a FFH 8-ary NCFSK system is presented for two cases: partial-band noise with broad-band noise, and tone jamming with broad-band noise. Results are generated by computer simulation for $L = 1, ..., 32$.

Order-statistic diversity combining is discussed in [9], and [25]-[27]. In [25], the probability of error for a FFH binary NCFSK system is derived for partial-band noise with broad-band noise. Results are presented for $L = 1, ..., 8$. In [9], the probability of error for a FFH 8-ary NCFSK system is presented for two cases: broad-band noise, and multiple-tone jamming with broad-band noise. Results are generated by computer simulation for $L = 1, ..., 32$. In [26], the probability of error for a FFH 8-ary NCFSK system is presented for two cases: broad-band noise, and multiple-tone jamming. Results are generated by computer simulation for $L = 1, ..., 32$. In [27], the probability of error for a FFH 8-ary NCFSK system is presented for two cases: broad-band noise, and multiple-tone jamming with broad-band noise. Results are generated by computer simulation for $L = 1, ..., 32$.

Weighted-order-statistic combining is discussed in [8] and [27]. In [8], the probability of error for a FFH M-ary NCFSK system is presented for partial-band noise with broad-band noise. Results are generated by computer simulation for $M = 2, 4, 8, 16$ and $L = 1, 3$. In [27], the probability of error for a FFH 8-ary NCFSK system is presented for two cases: broad-band noise, and multiple-tone jamming with broad-band noise. Results are generated by computer simulation for $L = 1, ..., 32$.

OSSNE combining is discussed in [26] and in [27]. In both papers, the probability of error for a FFH 8-ary NCFSK system is presented for two cases: broad-band noise, and multiple-tone jamming with broad-band noise. Results are generated by computer simulation for $L = 1, ..., 32$.

WOSSNE combining is discussed in [27]. The probability of error for a FFH 8-ary NCFSK system is presented for two cases: broad-band noise, and multiple-tone jamming with broad-band noise. Results are generated by computer simulation for $L = 1, ..., 32$.

Recursive-excision combining is discussed in [27]. The probability of error for a FFH 8-ary NCFSK system is presented for two cases: broad-band noise, and multiple-tone jamming with broad-band noise. Results are generated by computer simulation for $L = 1, ..., 32$.

Some observations pertaining to the use of the various diversity-combining methods in the demodulation of FFH NCFSK systems are presented. Optimum diversity combining is not a practical method because it involves estimation of signal and noise powers. Selection diversity combining is not a practical method because it is susceptible to partial-band interference. Clipped-linear, clipped-square-law, ratio-threshold-square-law, and ratio-threshold-majority-logic diversity combining are not practical methods because side information is required to set a clipping level or a threshold. Hard-decision-majority-vote di-

versity combining is not a good method because it does not utilize all the information from the matched-filter output samples. 4-2-moment-method, 2-1-moment-method, and 1-1/2-moment-method diversity combining perform poorly in fading. Linear diversity combining is an excellent method in broad-band noise. Square-law diversity combining is an excellent method in fading. Ratio-statistic-envelope, self-normalized-envelope, ratio-statistic-square-law, self-normalized-square-law, order-statistic, weighted-order-statistic, OSSNE, OSHDMV, WOSSNE, and recursive-excision diversity combining are excellent methods in multiple-tone jamming. The methods based on order statistics are computationally intensive. Linear, square-law, ratio-statistic-envelope, self-normalized-envelope, ratio-statistic-square-law, self-normalized-square-law, order-statistic, weighted-order-statistic, OSSNE, OSHDMV, WOSSNE, and recursive-excision diversity combining are all possible methods of choice.

2.6 Uplink Coarse-Time Synchronization for a FFH NCFSK Satellite-Communication System

The overall uplink coarse-time synchronization system for a particular FFH NCFSK satellite-communication systems is shown in Fig. 2.5. In this application, the transmitter of Fig. 2.1 is used to send a series of synchronization-probe bursts in a serial-search process. Onboard the satellite, the payload processor makes a decision as to whether a probe burst has been received. Only the probe bursts falling within the onboard hop-pattern window can be detected. An acknowledgement is sent back to the originating terminal for use in adjusting the hop-pattern timing. Synchronization-search strategies are considered elsewhere [28],[31]. Once coarse-time synchronization has been achieved, fine-time synchronization aligns the two hop periods to within the required tolerance [28],[34],[35].

The synchronization probe, shown in Fig. 2.6, consists of a tone at a frequency, $f_{hi}+f_p$, for the ith hop period. The probe frequency, f_p, is usually chosen as one of the M frequencies of the M-ary NCFSK channel so that no additional hardware is required. In Fig. 2.6, the probe arrives at the receiver with a timing error of ΔT relative to the onboard hop pattern. The dehopping process gates and downconverts the probe so that only the section of the probe falling within the onboard dehop period is seen at the output of the dehopper. If $|\Delta T|$ is greater than T_h, there is no probe energy available.

Following the dehopper is a bank of $E+1$ matched filters and envelope detectors of the form shown in Fig. 2.3. One filter is matched to the probe frequency, f_p, and E are

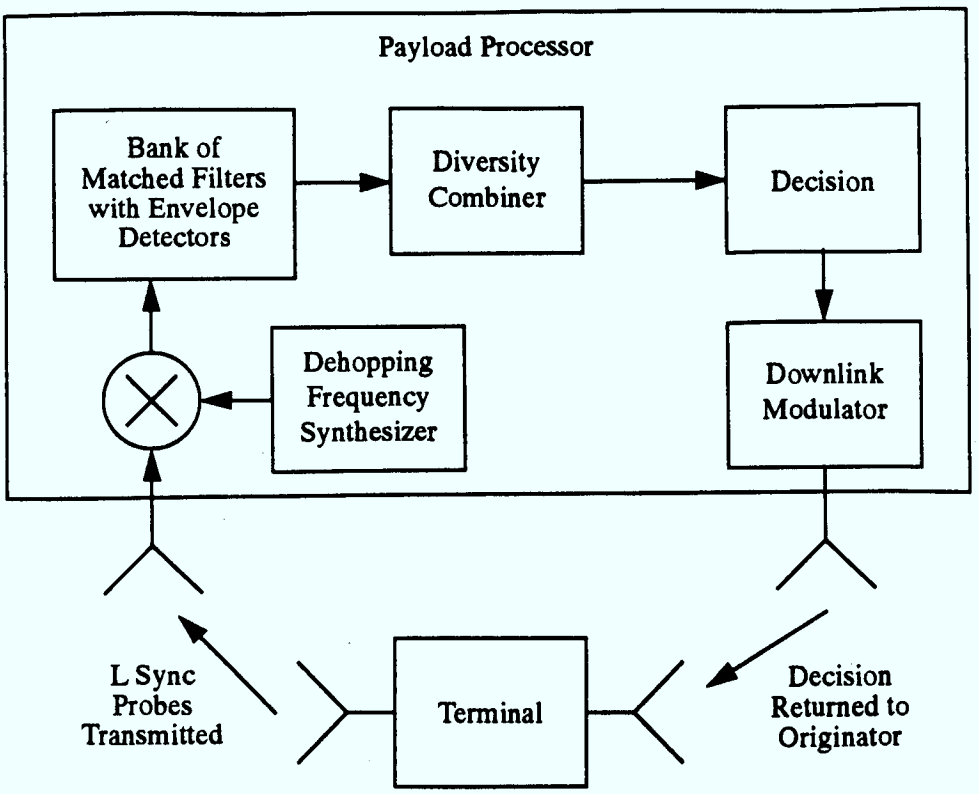

Figure 2.5: Simplified coarse-time synchronization system.

matched to frequencies other than the probe frequency. The outputs are the sampled values, z_{pi} and z_{ei}, for $i = 1, ..., L$, and $e = 1, ..., E$. The empty bins are used to obtain noise and interference statistics. The diversity combiner forms decision statistics, v_p and v_e for $e = 1, ..., E$, using one of the diversity-combining methods described previously. The decision statistics are then used to make the decision as to whether a detection has been made.

2.7 Summary

This chapter has provided the background in modulation and demodulation for FFH NCFSK systems with time diversity and diversity combining. A literature review of the various diversity-combining methods has been presented. For demodulation in FFH NCFSK systems, linear, square-law, ratio-statistic-envelope, self-normalized-envelope, ratio-statistic-square-law, self-normalized-square-law, order-statistic, weighted-order-statistic, OSSNE, OSHDMV, WOSSNE, and recursive-excision diversity combining are all possible

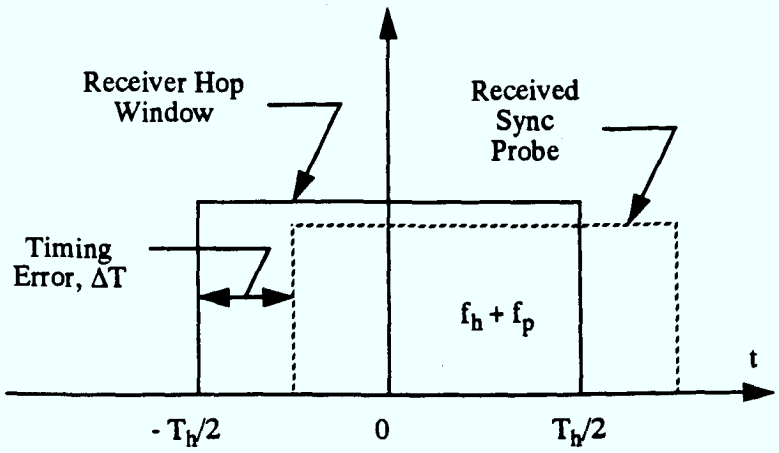

Figure 2.6: The gating of the dehopper.

methods of choice.

This chapter has also provided the background in uplink coarse-time synchronization for a FFH NCFSK satellite-communication system.

Since linear diversity combining is an excellent method for demodulation of FFH NCFSK systems in broad-band noise, it merits further study. In the next chapter, a novel analytical technique is derived which can be used to obtain performance results for demodulation of FFH NCFSK systems with time diversity and linear diversity combining and for the uplink coarse-time synchronization of a FFH NCFSK satellite-communication system.

Chapter 3

Analysis Method for Linear Combining

3.1 Introduction

A receiver often used in communications and radar is shown in Fig. 3.1. The input, $x(t)$, can be modelled as one or more tones plus AWGN. The tones, if present, can be a desired signal or interference. The receiver is assumed not to have knowledge of the phase of the desired signal. The desired signal has a basic period of duration, T. This input is applied to a filter noncoherently matched to the desired-signal frequency and then sampled at intervals of T to generate a complex sample, $\tilde{y}_i$, in the ith interval. Envelope detection is then performed to generate the envelope sample, z_i. Finally, L samples over the period LT are added together in an operation sometimes called "linear diversity combining" or just "linear combining", to obtain the decision statistic, v. The term "linear" refers to the sample combining, and not to the envelope-detection process which is actually nonlinear. This distinction is important since it is common practice to replace the envelope detector with a square-law detector. Unfortunately, this second type of combining is often misnamed "square-law combining" even though the actual combining is linear.

In order to analyze the performance of such a system, it is required to derive the probability density function (pdf) and cumulative distribution function (cdf) of the L-sample sum. There has been considerable previous work in deriving the pdf and cdf for the process where a square-law detector is used in place of the envelope detector. Much less has been done for envelope detection. In this chapter, a method of analysis is

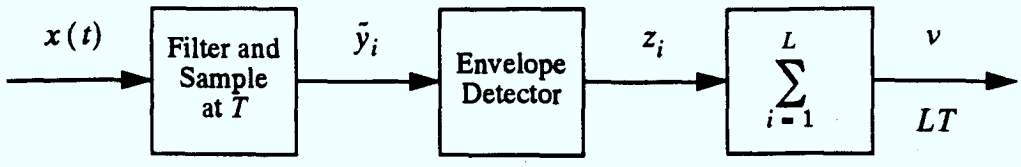

Figure 3.1: Simplified block diagram of process to be analyzed.

described that provides the pdf and cdf for the output, v, of the envelope detector and linear combiner of Fig. 3.1.

In previous work on envelope detection with linear combining, the pdf and cdf of the sum have been derived for some special cases of the stochastic process, $x(t)$. Brennan [36] computed the cdf of the sum of independent Rayleigh random variables, which occur if the input, $x(t)$, consists of white Gaussian noise, by doing repeated convolutions using numerical integration. Marcum [37] derived a method of evaluating the cdf of the sum of independent Rayleigh random variables, and of the sum of independent Rician random variables, which occur if the input, $x(t)$, consists of a sine wave plus white Gaussian noise, using Gram-Charlier series. Beaulieu [38] derived an efficient way of evaluating the pdf and cdf of the sum of independent Rayleigh random variables using Fourier series. Helstrom [39] derived a method of evaluating the pdf and cdf of the sum of independent Rayleigh and the sum of independent Rician random variables using Laplace transforms and saddlepoint integration. These methods either are not general enough to cover all cases of interest or are very difficult and labourious to implement computationally.

In this chapter, the technique developed by Bird [40] to analyze the pdf for a single sample using circularly symmetric function theory and Fourier-Bessel series is combined with a method [38],[41] which uses Fourier series to analyze the pdf and cdf of the sum of independent random variables in order to provide a method of analysis that is capable of calculating the pdf and cdf of the decision statistic, v. This method is not only computationally efficient and accurate, but is applicable to more general problems.

Once the pdf and cdf have been found, a variety of performance values can be determined. In particular, it can be used for computing the probability of error in demodulation problems, the probability of detection and false alarm in detection problems, and the mean and variance of estimates in estimation problems.

This method can be used to obtain performance measures for FFH NCFSK systems.

For demodulation of the dehopped signal in a general FFH NCFSK system [15],[19],[28], there are M branches with M outputs, v_m, for $m = 1, ..., M$, as shown in Fig. 3.2. The largest value is selected as corresponding to the symbol received. For coarse-time-synchronization algorithms that require the detection of synchronization probes, there is at least one branch like that in Fig. 3.1 to detect the probes, and possibly others to sample the interference background [28]-[33]. For fine-time-synchronization algorithms that employ synchronization probes, two or more branches are used, and the outputs, v_m, are used to calculate an estimate of the timing error [28],[34],[35]. In this report, the analysis method is applied to diversity combining for the demodulation of FFH NCFSK systems and for uplink coarse-time synchronization of a FFH NCFSK satellite-communication system.

3.2 Mathematical Approach

Consider the general block diagram shown in Fig. 3.2. Let the input consist of a signal tone, plus one or more interfering tones, plus white Gaussian noise. In the ith transmission interval of duration, T, a sample is taken in every branch. Then, L of these are accumulated over the total symbol period LT. The output of the mth branch is

$$v_m = \sum_{i=1}^{L} z_{mi} \tag{3.1}$$

where z_{mi} is the envelope sample for the mth branch during the ith interval. To find the pdf and cdf of v_m, the pdf of z_{mi} is derived first.

Let the signal tone at the mth branch be

$$\sqrt{2} s_{mi} \cos(2\pi f_m t + \phi_{mi}) \tag{3.2}$$

where s_{mi} is the rms amplitude, f_m is the frequency, and ϕ_{mi} is a random phase angle. The interference tone is

$$\sqrt{2} a_{mi} \cos(2\pi f_m t + \alpha_{mi}) \tag{3.3}$$

where a_{mi} is the rms amplitude, f_m is the frequency, and α_{mi} is a random phase angle. The noise is a white Gaussian random process with zero mean and two-sided noise power-spectral density, $N_0/2$. The sum of these three signals passes through the matched filter and envelope detector of Fig. 2.4.

The output sample of the matched filter with envelope detector, z_{mi}, is the magnitude of a two-dimensional vector. This vector can be written as a complex number, $\tilde{y}_{mi}$, where

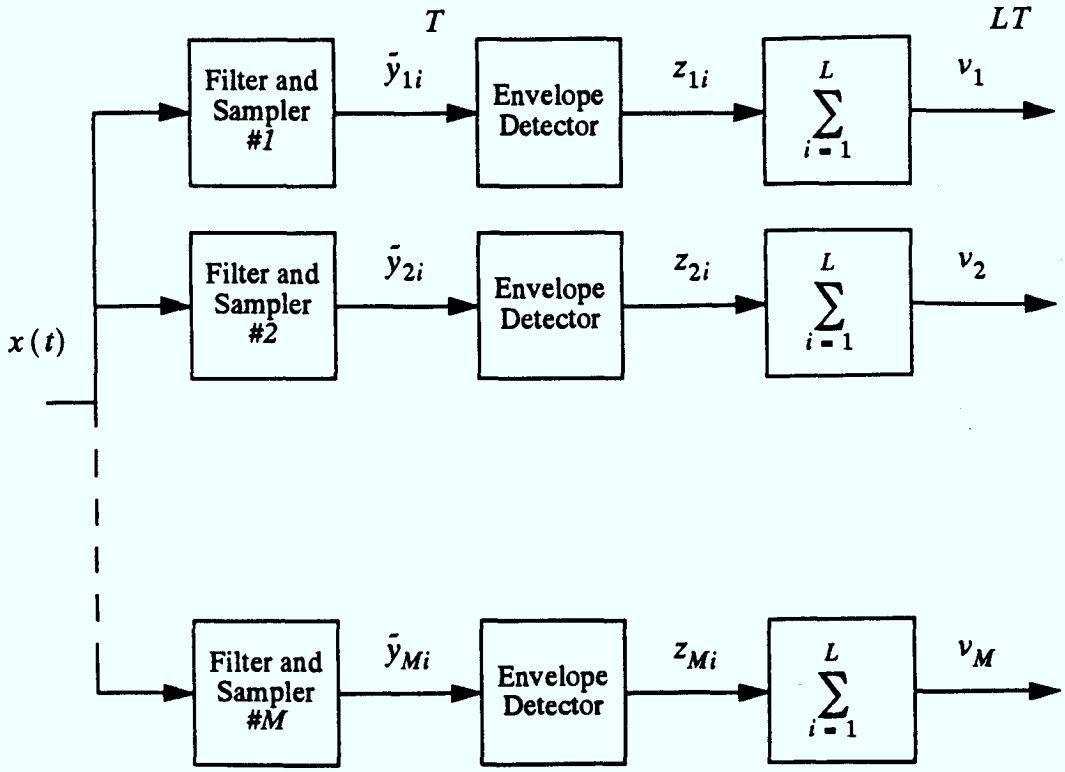

Figure 3.2: A block diagram of the basic process with M branches.

the real part, y_{mic}, is the sampled output of the in-phase integrator, and the imaginary part, y_{mis}, is the sampled output of the quadrature integrator. Then, $\tilde{y}_{mi}$ is

$$\tilde{y}_{mi} = y_{mic} + jy_{mis} = \tilde{s}_{mi} + \tilde{a}_{mi} + \tilde{n}_{mi} \tag{3.4}$$

so that

$$\tilde{s}_{mi} = s_{mi}\cos(\phi_{mi}) + js_{mi}\sin(\phi_{mi}), \tag{3.5}$$

$$\tilde{a}_{mi} = a_{mi}\cos(\alpha_{mi}) + ja_{mi}\sin(\alpha_{mi}), \tag{3.6}$$

$$\tilde{n}_{mi} = n_{mic} + jn_{mis}. \tag{3.7}$$

It can be shown that the noise components, n_{mic} and n_{mis}, are Gaussian random variables with zero mean and variance,

$$\sigma^2 = \frac{N_0}{2T}. \tag{3.8}$$

The pdf of $z_{mi} = |\tilde{y}_{mi}|$ is [40]

$$f_{z_{mi}}(z_{mi}) = \int_0^\infty z_{mi}\rho J_0(\rho z_{mi})\Phi_{\tilde{y}_{mi}}(\rho)d\rho \tag{3.9}$$

where $\Phi_{\tilde{y}_{mi}}(\rho)$ is the two-dimensional characteristic function of $\tilde{y}_{mi}$ given by [40]

$$\Phi_{\tilde{y}_{mi}}(\rho) = \int_0^\infty J_0(\rho z_{mi}) f_{z_{mi}}(z_{mi}) dz_{mi}, \tag{3.10}$$

and $J_0()$ is the zeroth-order Bessel function of the first kind. Since the random variable, $\tilde{y}_{mi}$, is the sum of independent components, the two-dimensional characteristic function of $\tilde{y}_{mi}$ is the product of the characteristic functions of its corresponding components. Therefore, the two-dimensional characteristic function of each component is required so that (3.9) can be used to find the pdf of z_{mi}.

For a constant signal tone of duration, T, the characteristic function is found from (3.10) as [40]

$$\Phi_{\tilde{s}_{mi}}(\rho) = J_0(\rho s_{mi}). \tag{3.11}$$

For a constant interference tone of duration, T, the characteristic function is [40]

$$\Phi_{\tilde{a}_{mi}}(\rho) = J_0(\rho a_{mi}). \tag{3.12}$$

The characteristic function for the noise is [40]

$$\Phi_{\tilde{n}_{mi}}(\rho) = exp(-\frac{\sigma^2\rho^2}{2}). \tag{3.13}$$

The characteristic function of $\tilde{y}_{mi}$ is

$$\Phi_{\tilde{y}_{mi}}(\rho) = \Phi_{\tilde{s}_{mi}}(\rho)\Phi_{\tilde{a}_{mi}}(\rho)\Phi_{\tilde{n}_{mi}}(\rho). \tag{3.14}$$

The pdf of z_{mi} can be found by substituting (3.14) into (3.9). Unfortunately, the integral in (3.9) cannot usually be solved analytically for most signal combinations of interest. Previous work in evaluating the pdf and cdf of z_{mi} has followed three different approaches. The first approach leads to series solutions in terms of Laguerre polynomials [42]-[44]. The second involves numerical integration [45],[46]. These two approaches are complicated and specialized to each individual problem. The third uses Fourier-Bessel series which leads to an efficient numerical solution. It can be shown that [40]

$$f_{z_{mi}}(z_{mi}) = 2z_{mi} \sum_{q=1}^{\infty} \frac{\Phi_{\tilde{y}_{mi}}(\lambda_q/R)}{[J_1(\lambda_q)]^2 R^2} J_0(\frac{\lambda_q z_{mi}}{R}) \tag{3.15}$$

where λ_q are the zeroes of $J_0()$ for $q = 1, 2, ..., \infty$ in ascending order, and R is a value chosen such that for $z_{mi} > R$, $f_{z_{mi}}(z_{mi})$ is sufficiently close to zero. The cdf of z_{mi} can be obtained by integrating (3.15) with respect to z_{mi} term by term leading to [40]

$$F_{z_{mi}}(z_{mi}) = 2z_{mi} \sum_{q=1}^{\infty} \frac{\Phi_{\tilde{y}_{mi}}(\lambda_q/R)}{[J_1(\lambda_q)]^2 R\lambda_q} J_1(\frac{\lambda_q z_{mi}}{R}). \tag{3.16}$$

Thus, both the cdf and pdf of z_{mi} can be efficiently evaluated using Fourier-Bessel series.

There are two types of truncation error involved with evaluating (3.15) or (3.16). It is necessary to truncate the series after Q terms and to choose a value of R. For a signal with tone interference and Gaussian noise, it is suggested in [40] that R be chosen to be

$$R = R_I + 10\sigma \tag{3.17}$$

where R_I is the sum of the rms amplitudes of the signal and interfering tones. This selection makes the truncation error due to the choice of R negligible [40]. Then, Q is chosen so that the truncation error due to the finite series is sufficiently small. In order to guarantee a sufficiently small truncation error, calculations of the pdf and cdf are repeated with increasing numbers of terms in the series of (3.15) and (3.16) until the final results do not change by more than the required accuracy.

The pdf of z_{mi} is now used to determine the pdf and cdf of v_m given by (3.1). Note that the z_{mi} for $i = 1, ..., L$ are independent random variables. Beaulieu [38] and Bird [41] have provided similar means of determining the pdf and cdf of a sum of independent random variables. The technique used below more closely follows the approach of Beaulieu [38] with suitable modifications for the problem at hand.

In the derivation of (3.15), it is assumed that $f_{z_{mi}}(z_{mi}) = 0$ for $z_{mi} > R$ and also for $z_{mi} < 0$. Since v_m is the sum of the z_{mi}, it follows that the pdf of v_m, $f_{v_m}(v_m)$, is zero for $v_m > LR$ and also for $v_m < 0$. A typical $f_{v_m}(v_m)$ is shown in Fig. 3.3. Now from [38], the artifice is introduced of multiplying $f_{v_m}(v_m)$ by a square wave, $S_V(v_m - L\epsilon_m)$, also shown in Fig. 3.3. Here, $L\epsilon_m$ is a constant offset. The square wave is defined by

$$S_V(v) = \sum_{u=-\infty}^{u=\infty} \text{rect}\left(\frac{v - \frac{V}{2} - uV}{V}\right) \tag{3.18}$$

where

$$\text{rect}(v) = \begin{cases} 1, & |v| \leq 0.5, \\ 0, & |v| > 0.5. \end{cases} \tag{3.19}$$

The period of the square wave is chosen to be $V = 2LR$. The cdf of v_m is

$$F_{v_m}(\epsilon_m L) = \int_0^{\epsilon_m L} f_{v_m}(v)dv, \tag{3.20}$$

$$= 1 - \int_{\epsilon_m L}^{LR} f_{v_m}(v)dv, \tag{3.21}$$

Since $S_V(v - \epsilon_m L) = 1$ for $\epsilon_m L < v < LR$, and $S_V(v - \epsilon_m L) f_{v_m}(v) = 0$ for $v < \epsilon_m L$ and $v > LR$, (3.21) can be written as

$$F_{v_m}(\epsilon_m L) = 1 - \int_{\epsilon_m L}^{LR} S_V(v - \epsilon_m L) f_{v_m}(v)dv. \tag{3.22}$$

$$= 1 - \int_{-\infty}^{\infty} S_V(v - \epsilon_m L) f_{v_m}(v) dv. \tag{3.23}$$

$$= 1 - E[S_V(v_m - \epsilon_m L)] \tag{3.24}$$

where $E[\,]$ denotes expectation over the random variable, v_m. Thus, the cdf of v_m can be expressed in terms of the expected value of the periodic square wave. Note that (3.24) is true if $f_{v_m}(v_m)$ does not have an impulse at a discontinuity of $S_V(v_m - \epsilon_m L)$ [38].

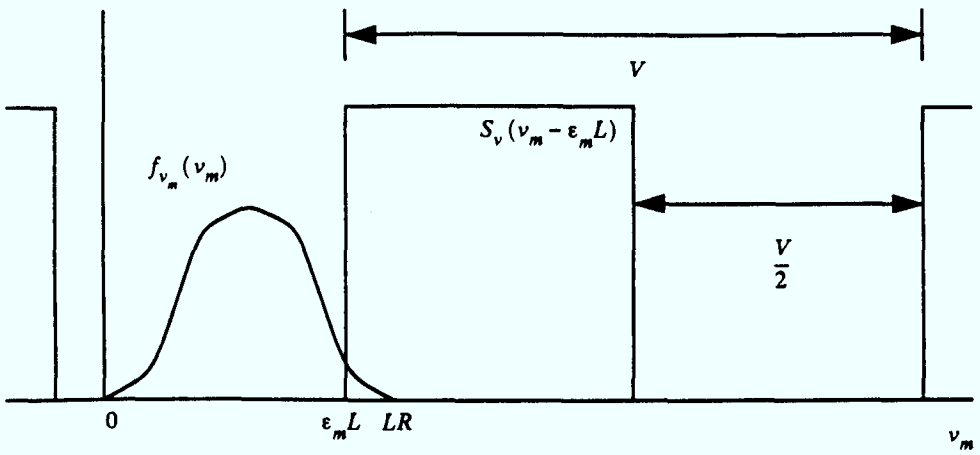

Figure 3.3: The pdf of v_m.

The Fourier series representation of $S_V(v)$ is [38]

$$S_V(v) = \frac{1}{2} + \sum_{k=-\infty, k odd}^{k=\infty} \frac{e^{jk\omega v}}{\pi k j} \tag{3.25}$$

where $\omega = 2\pi/V$. Combining (3.24) and (3.25) gives [38]

$$F_{v_m}(\epsilon_m L) = \frac{1}{2} - \sum_{k=-\infty, k odd}^{k=\infty} \frac{E[e^{jk\omega(v_m - \epsilon_m L)}]}{\pi k j}. \tag{3.26}$$

After considerable algebraic manipulation, the pdf and cdf of v_m can be found from the pdf of z_{mi} by the Fourier series expansion and are given by [38]

$$F_{v_m}(v_m) = \frac{1}{2} - \frac{2}{\pi} \sum_{k=1, k\ odd}^{\infty} \frac{A_{mk} \sin \theta_{mk}}{k}, \tag{3.27}$$

$$f_{v_m}(v_m) = \frac{4}{V} \sum_{k=1, k\ odd}^{\infty} A_{mk} \cos \theta_{mk} \tag{3.28}$$

where

$$A_{mik} = \sqrt{(E[\cos(k\omega z_{mi})])^2 + (E[\sin(k\omega z_{mi})])^2}, \tag{3.29}$$

$$\theta_{mik} = \tan^{-1}\left(\frac{E[\sin(k\omega(z_{mi} - \epsilon_m))]}{E[\cos(k\omega(z_{mi} - \epsilon_m))]}\right), \tag{3.30}$$

$$A_{mk} = \prod_{i=1}^{L} A_{mik}, \tag{3.31}$$

$$\theta_{mk} = \sum_{i=1}^{L} \theta_{mik}, \tag{3.32}$$

$$\epsilon_m = \frac{v_m}{L}. \tag{3.33}$$

Beaulieu [38] has shown that the series in (3.27) and (3.28) converge. The expected values, $E[\cos(k\omega z_{mi})]$ and $E[\sin(k\omega z_{mi})]$, are calculated by

$$E[\cos(k\omega z_{mi})] = \int_0^R \cos(k\omega z_{mi}) f_{z_{mi}}(z_{mi}) dz_{mi} \tag{3.34}$$

and

$$E[\sin(k\omega z_{mi})] = \int_0^R \sin(k\omega z_{mi}) f_{z_{mi}}(z_{mi}) dz_{mi} \tag{3.35}$$

using numerical integration where $f_{z_{mi}}(z_{mi})$ is given by (3.15). The coefficients, A_{mk} and θ_{mk}, can be found from (3.29)-(3.35). The choice of $V = 2LR$ simplifies the computations since the numerical integrations of (3.34) and (3.35) need only be evaluated once for each value of k for any given pdf. The pdf and the cdf of v_m can then be found using (3.27) and (3.28). The series in (3.27) and (3.28) are truncated after K terms. Note that $(K-1)/2$ terms are zero because the summation is only over odd terms. Thus, to calculate the pdf and cdf of v_m, only $K+1$ single integrations are needed. In order to guarantee a sufficiently small truncation error, calculations of the pdf and cdf are repeated with increasing numbers of terms in the series of (3.27) and (3.28) until the final results do not change by more than the required accuracy.

3.3 Comparison with Other Results

In this section, a comparison is made between the numerical results generated using the above method and previously published results.

3.3.1 Sum of Five Rayleigh Random Variables

Consider the problem of finding the cdf of the sum of five Rayleigh random variables, z_{mi}, for $i = 1, ..., 16$, where each random variable has a pdf of

$$f_{z_{mi}}(z_{mi}) = z_{mi} \exp(\frac{-z_{mi}^2}{2}), z_{mi} \geq 0. \tag{3.36}$$

Beaulieu [38] has shown that for the Rayleigh random variable of (3.36), the integrals of (3.34) and (3.35) are

$$E[\cos(k\omega z_{mi})] = {}_1F_1(1, \frac{1}{2}, -\frac{k^2\omega^2}{2}), \tag{3.37}$$

$$E[\sin(k\omega z_{mi})] = \sqrt{\frac{\pi}{2}} k\omega \exp(-\frac{k^2\omega^2}{2}) \tag{3.38}$$

where ${}_1F_1(,,)$ is the confluent hypergeometric function. The cdf of the sum can then be found from (3.27). Beaulieu [38] shows an efficient way of evaluating (3.37). The series of (3.27) must be truncated after a certain number of terms. The cdf was computed with various numbers of terms, and the results are shown in Table 3.1 along with the previously published results of Helstrom [39]. Note that there is agreement to 6 decimal places between the results with 30 terms and 40 terms; therefore, 30 terms are sufficient for an accuracy of $\pm 10^{-6}$. In addition, the results of [39] and those calculated in this report agree.

v_m	20 terms	30 terms	40 terms	Helstrom [39]
1.0	-0.000046864425	0.000000087051	0.000000242536	0.000000246072
3.0	0.006013209643	0.006040403871	0.006040461398	0.00604046
5.0	0.198147788091	0.198135172457	0.198135073842	0.198135
6.0	0.446517392095	0.446545531179	0.446545628911	0.446546
7.0	0.702846895639	0.702811444082	0.702811389564	0.702811
9.0	0.961571441004	0.961548568638	0.961548621161	0.9615486
11.0	0.998229594502	0.998237077575	0.998237134497	0.99823713
13.0	0.999946637776	0.999969488835	0.999969472545	0.9999694733

Table 3.1: The CDF of 5 Rayleigh Random Variables

3.3.2 Sum of Sixteen Rician Random Variables

Consider the problem of finding the cdf of the sum, v_m, of sixteen Rician random variables, z_{mi}, for $i = 1, ..., 16$, where each random variable has the pdf,

$$f_{z_{mi}}(z_{mi}) = z_{mi} \exp(\frac{-z_{mi}^2 + s_{mi}}{2}) I_0(z_{mi} s_{mi}), z_{mi} \geq 0. \quad (3.39)$$

In this case, the integrals in (3.34) and (3.35) cannot be solved analytically. Numerical integration was used employing the adaptive-Romberg algorithm [47]. The integration was stopped when the error was less than a fraction, $\delta = 10^{-8}$, of the value of the integral. The cdf was computed with various numbers of terms, and the results are shown in Table 3.2 along with the previously published results of Helstrom [39]. Note that there is agreement to 8 decimal places between the results with 50 terms and 70 terms; therefore, 50 terms are sufficient for an accuracy of $\pm 10^{-8}$. In addition, the results of [39] and those calculated in this report agree.

s_{mi}	30 terms	50 terms	70 terms	Helstrom [39]
1.2604192	0.932001282965	0.932011262474	0.932011262683	0.9320114
1.5867737	0.644568109834	0.644600482984	0.644600482906	0.644601
1.9976298	0.134545925833	0.134562469337	0.134562469396	0.134563
2.5148669	0.001217999774	0.001246864269	0.001246864363	0.00124687

Table 3.2: The CDF of 16 Rician Random Variables

3.4 Summary

A method for obtaining the pdf and the cdf of a sum of independent random variables has been presented. The method is independent of the underlying pdf. An efficient way of evaluating the pdf and the cdf of the sum has been provided. The cdf computed using this method has been compared to the cdf computed using a previously known method, and the results agree well. This novel analytical technique can be used to obtain performance results for systems employing linear combining. The application is demonstrated in the next two chapters.

Chapter 4

Application to Demodulation of FFH NCFSK Systems

4.1 Introduction

Previous error-performance analyses for FFH M-ary NCFSK receivers with linear diversity combining have primarily used computer simulation [2],[4],[8],[9] or approximations [6]. However, Keller [7] calculates the probability of bit error, P_b, in partial-band noise using an analytical method based on repeated convolutions which is only practical for small levels of diversity and cannot be used for multiple-tone interference. An analytical method is needed to compute P_b for an arbitrary level of diversity for the following situations: 1) partial-band-noise jamming plus system noise, 2) multiple-tone jamming plus system noise, and 3) fading plus system noise. This chapter presents the application of the analytical method presented in the last chapter to the demodulation problem in FFH M-ary NCFSK systems with linear diversity combining.

Previous error-performance analyses for FFH M-ary NCFSK receivers with 2-1- and 4-2-moment-method diversity combining have primarily used computer simulation [9],[19],[20]. This chapter presents an analytical method for the FFH binary NCFSK demodulation problem with 2-1- and 4-2-moment-method diversity combining and $L = 2$ in independent Rayleigh fading.

4.2 Broad-Band Noise

The probability of bit error was calculated for various levels of diversity in broad-band AWGN. The noise can originate from both system noise and jamming. The signal-to-noise ratio after dehopping is given by

$$SNR = \frac{E_h}{N_0} = \frac{s_{mi}^2}{2\sigma^2} \tag{4.1}$$

where E_h is the energy per hop, $N_0/2$ is the two-sided noise power-spectral density, and $\sigma^2 = N_0/2T_h$. This SNR is appropriate for a fixed-hop-rate system. Perfect time synchronization and frequency synchronization are assumed. The probability of symbol error is given by

$$P_s = 1 - \int_0^\infty [F_n(v)]^{M-1} f_{sn}(v) dv \tag{4.2}$$

where $F_n(v)$ is the cdf of the decision statistic with only broad-band noise present, and $f_{sn}(v)$ is the pdf of the decision statistic with broad-band noise and a signal tone present. The probability of bit error is then

$$P_b = \frac{M}{2(M-1)} P_s. \tag{4.3}$$

Therefore, the calculation of P_b requires only a single integration. The adaptive-Romberg method was used for the numerical integration [47] with $\delta = 10^{-8}$. To calculate the Fourier-Bessel series of (3.15) and (3.16), 150 terms were used. To calculate the Fourier series of (3.27) and (3.28), 40 nonzero terms were used. With the above choices, the results have an accuracy of $\pm 10^{-8}$.

The probability of bit error was calculated for various levels of diversity in broad-band AWGN for linear combining with the same parameters as in [19] where results are generated by computer simulation; therefore, $M = 8$ and $SNR = -0.2$ dB. From (4.2) and (4.3), the probability of bit error was calculated for various levels of diversity and is plotted in Fig. 4.1. The results generated in this report agree with the results presented in [19]. Note that the probability of bit error decreases as the level of diversity is increased.

Since linear and square-law combining are near-optimal diversity-combining schemes in broad-band AWGN, a comparison between the two would be interesting. The probability of bit error with $M = 2$ for square-law combining is given by [55]

$$P_b = \frac{1}{2^{2L-1}} \exp(-\frac{LE_h}{2N_0}) \sum_{n=0}^{L-1} c_n (\frac{LE_h}{2N_0})^n \tag{4.4}$$

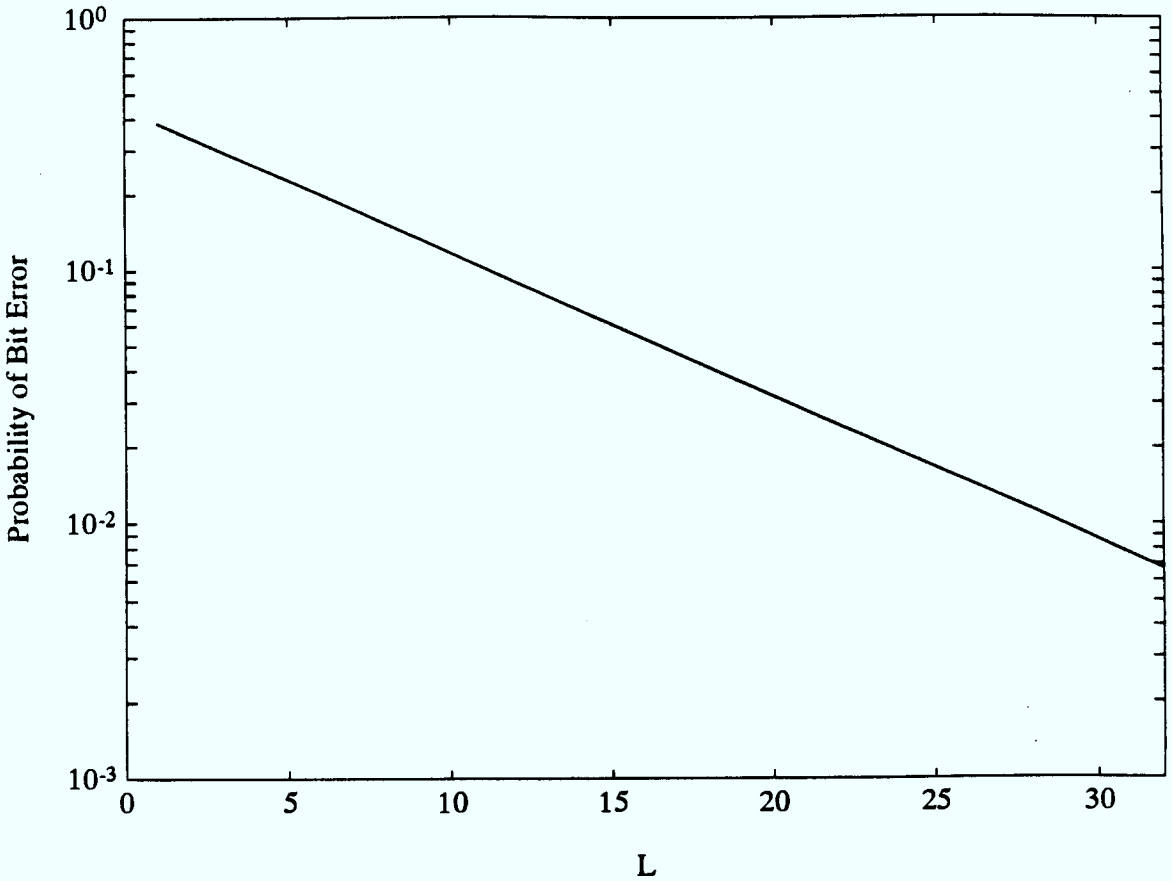

Figure 4.1: P_b with $M = 8$ and $SNR = -0.20$ dB in broad-band noise.

where

$$c_n = \frac{1}{n!} \sum_{k=0}^{L-1-n} \binom{2L-1}{k}. \tag{4.5}$$

Table 4.1 shows the performance of the two diversity-combining methods with $SNR = -5$ dB and $SNR = 0$ dB. The P_b is almost the same for both methods. Thus, linear and square-law combining have similar performance. Recall that linear combining has near-optimal performance for large SNR in broad-band AWGN and that square-law combining has near-optimal performance for small SNR in broad-band AWGN. Then, both combining methods have near-optimal performance independent of the signal-to-noise ratio.

SNR in dB	L	P_b for square law	P_b for linear
0	8	0.069145	0.068921
0	12	0.034761	0.034492
0	16	0.018060	0.017842
0	20	0.009571	0.009414
0	24	0.005141	0.005035
0	28	0.002788	0.002719
0	32	0.001523	0.001479
-5	8	0.289804	0.293143
-5	12	0.248320	0.252187
-5	16	0.216027	0.220198
-5	20	0.189728	0.194068
-5	24	0.167742	0.172158
-5	28	0.149040	0.153467
-5	32	0.132937	0.137328

Table 4.1: P_b with $M = 2$ in Broad-band Noise

4.3 Multiple-Tone Jamming

The probability of bit error was calculated for binary NCFSK with $L = 8$ in multiple-tone jamming plus broad-band AWGN for two types of jamming strategies. First, results are presented for randomly distributed multiple-tone jamming. Then, these results are compared to results for Houston-sense multiple-tone jamming.

4.3.1 Randomly Distributed Multiple-Tone Jamming

For randomly distributed multiple-tone jamming, the jammer tones are randomly located in a fraction, γ, of the total number of bins. All jammer tones are of the same amplitude, a_{mi}. Each jamming tone is assumed to be at the centre of the frequency bin. The signal-to-noise ratio is given by (4.1). The ratio of signal to tone jammer after dehopping is given by

$$SJR = \frac{E_h}{J_o} = \frac{s_{mi}^2}{\gamma a_{mi}^2} \tag{4.6}$$

where E_h is the energy per hop, and J_o is the equivalent jammer power-spectral density. For L hops, the bin with the desired signal will contain a signal tone plus noise every time, but would contain a jammer tone l_s times where l_s is a random integer with $0 \leq l_s \leq L$. Similarly, for L hops, the empty bin would contain noise every time, but would contain a jammer tone l_e times where l_e is a random integer with $0 \leq l_e \leq L$. The probability of each combination of tone jamming can be calculated from

$$P_{comb}(l_s, l_e) = \binom{L}{l_s}\binom{L}{l_e}\gamma^{l_s+l_e}(1-\gamma)^{2L-l_s-l_e}. \tag{4.7}$$

The probability of a correct decision for each combination of tone jamming, $P_{correct}(l_e, l_s)$, is calculated using

$$P_{correct}(l_e, l_s) = \int_0^\infty F_e(v) f_s(v) dv \tag{4.8}$$

where $f_s()$ is the pdf of the signal-bin decision statistic, and $F_e()$ is the cdf of the empty-bin decision statistic. The overall probability of a correct decision is then

$$P_{correct} = \sum_{l_s=0}^{L}\sum_{l_e=0}^{L} P_{comb}(l_e, l_s) P_{correct}(l_e, l_s), \tag{4.9}$$

and P_b is

$$P_b = 1 - P_{correct}. \tag{4.10}$$

From (4.7)-(4.10), P_b was calculated for $SNR = 10$ dB and for various SJR, and is plotted as a functions of γ in Fig. 4.2. The adaptive-Romberg method was used for the numerical integration [47] with $\delta = 10^{-8}$. To calculate the Fourier-Bessel series of (3.15) and (3.16), 150 terms were used. To calculate the Fourier series of (3.27) and (3.28), 200 nonzero terms were used. With the above choices, the results have an accuracy of $\pm 10^{-8}$.

For $SNR = 10$ dB and $SJR = -5$ dB, P_b is at a maximum of 0.2910 for a jamming fraction of $\gamma = 1.0$. As γ approaches zero, P_b drops considerably. Thus, jamming all the bins is the most detrimental jamming strategy at this level of interference.

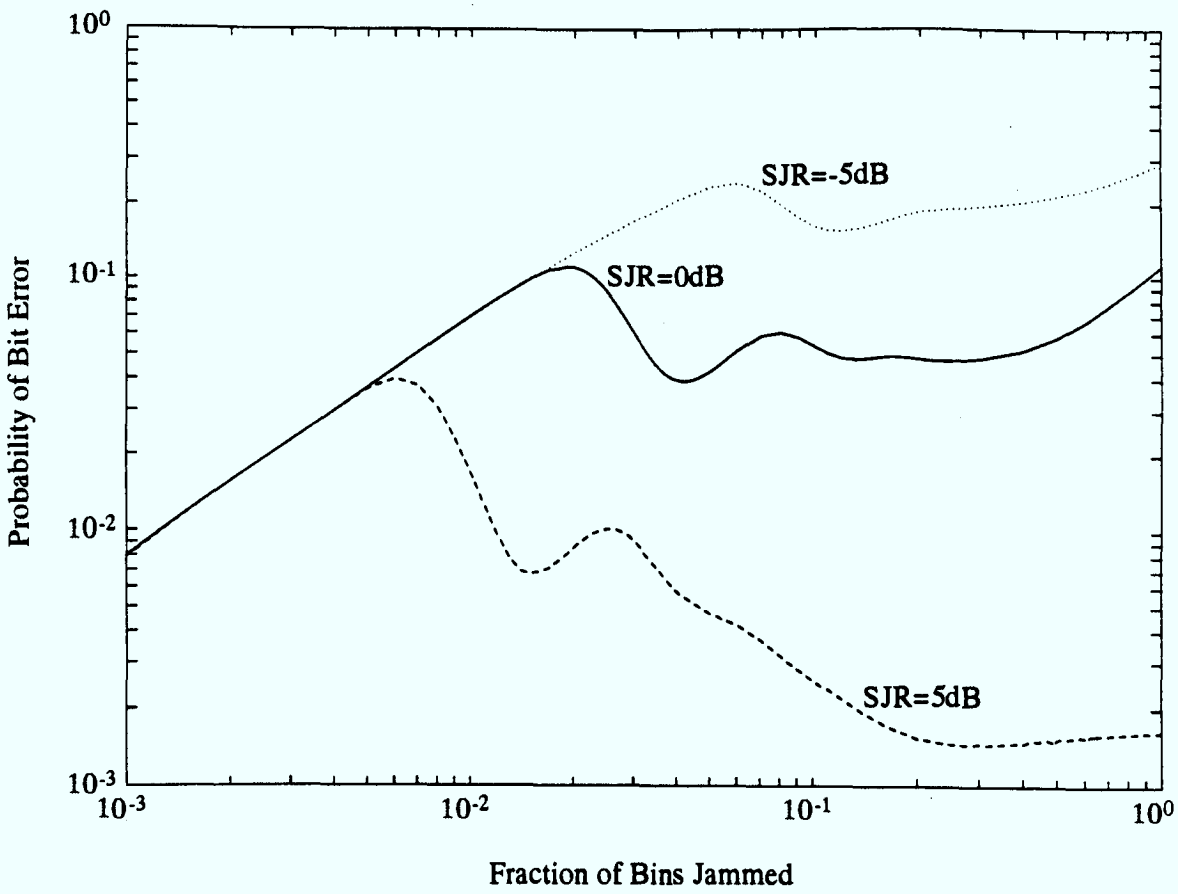

Figure 4.2: P_b for randomly distributed multiple-tone jamming, $L = 8$, $M = 2$, $SNR = 10$ dB.

For $SNR = 10$ dB and $SJR = 0$ dB, P_b is at a maximum of 0.1127 for a jamming fraction of $\gamma = 0.019$. As γ approaches zero, P_b drops considerably. Note that $P_b = 0.1123$ for $\gamma = 1.0$. Thus, jamming all the bins is almost as detrimental as jamming the worst-case fraction of bins at this level of interference.

For $SNR = 10$ dB and $SJR = 5$ dB, P_b is at a maximum of 0.0408 for a jamming fraction of $\gamma = 0.006$. As γ approaches zero, P_b drops considerably. For $\gamma = 1.0$, $P_b = 0.0016$. Thus, jamming with $\gamma = 0.006$ is much worse than jamming with $\gamma = 1.0$.

For $SJR = -5$ dB, the highest P_b occurs at full-band jamming. For $SJR = 0$ dB and $SJR = 5$ dB, the highest P_b occurs at a relatively small jamming fraction ($\gamma = 0.019$ and $\gamma = 0.006$ respectively). For small jamming fractions ($\gamma < 0.005$), P_b is almost the same for all three values of SJR. Full-band jamming is very detrimental at $SJR = 0$ dB and $SJR = -5$ dB, but is not the worst case for $SJR = 5$ dB.

4.3.2 Houston-Sense Multiple-Tone Jamming

For Houston-sense multiple-tone jamming, a fraction, α, of the total number of M-bin channels are jammed by placing a single jammer tone in the centre of one bin of that channel. Two jammer tones are never located in the same channel. This strategy was first discussed in [51] for situation without diversity. It is the worst-case jamming when diversity is not employed. The fraction, γ, of bins jammed is $\gamma = \alpha/M$. All jammer tones are of the same amplitude, a_{mi}. Each tone's centre is at the centre of the frequency bin. The signal-to-noise ratio is given by (4.1). The ratio of signal to tone jammer after dehopping is given by (4.6).

Consider a FFH binary ($M = 2$) NCFSK system. For L hops, the bin with the desired signal will contain a signal tone plus noise every time, but would contain a jammer tone l_s times where l_s is a random integer with $0 \leq l_s \leq L$. Similarly, for L hops, the empty bin would contain noise every time, but would contain a jammer tone l_e times where l_e is a random integer with $0 \leq l_e \leq L - l_s$. The probability of each combination of tone jamming can be calculated from

$$P_{comb}(l_s, l_e) = \binom{l_s + l_e}{l_s} \binom{L}{l_s + l_e} (\frac{1}{2})^{l_s+l_e} \alpha^{l_s+l_e} (1-\alpha)^{L-l_s-l_e}. \tag{4.11}$$

The probability of a correct decision for each combination of tone jamming, $P_{correct}(l_e, l_s)$, is calculated by (4.8) using (4.11). The overall probability of a correct decision is then calculated using (4.9), and P_b is given by (4.10). From (4.8)-(4.11), P_b was calculated for $SNR = 10$ dB and for $SJR = -5$ dB and $SJR = 0$ dB, and is plotted as a function of

γ in Fig. 4.3. The adaptive-Romberg method was used for the numerical integration [47] with $\delta = 10^{-8}$. To calculate the Fourier-Bessel series of (3.15) and (3.16), 150 terms were used. To calculate the Fourier series of (3.27) and (3.28), 200 nonzero terms were used. With the above choices, the results have an accuracy of $\pm 10^{-8}$.

For $SNR = 10$ dB and $SJR = -5$ dB, P_b is at a maximum of 0.2834 for a jamming fraction of $\gamma = 0.5$. As γ approaches zero, P_b drops considerably. Thus, jamming all the channels is the most detrimental jamming strategy at this level of interference.

For $SNR = 10$ dB and $SJR = 0$ dB, P_b is at a maximum of 0.1138 for a jamming fraction of $\gamma = 0.02$. As γ approaches zero, P_b drops considerably. Note that $P_b = 0.0996$ for $\gamma = 0.5$. Thus, jamming with $\gamma = 0.02$ is much worse than jamming with $\gamma = 0.5$.

For $SJR = -5$ dB, the highest P_b occurs at full-band jamming. For $SJR = 0$ dB, the highest P_b occurs at a relatively small jamming fraction ($\gamma = 0.02$). Houston-sense jamming is worse than randomly distributed jamming at $SJR = 0$ dB; however, randomly distributed jamming is worse than Houston-sense jamming at $SJR = -5$ dB. This second point is very important. It is often stated in the literature [9],[26],[27] that Houston-sense jamming is the worst case. However, for $L = 8$, $M = 2$, and $SJR = -5$ dB, this is not true. Thus, Houston-sense jamming is not necessarily the worst-case jamming.

4.4 Rayleigh Fading

In this section, the performance of linear, square-law, 4-2-moment method, and 2-1-moment-method diversity combining is considered in Rayleigh fading. Results are derived for $M = 2$ and $L = 2$.

4.4.1 The PDF for z_{mi} in Independent Rayleigh Fading

The output sample of the matched filter with envelope detector, z_{mi}, is the magnitude of a complex number,

$$\tilde{y}_{mi} = \tilde{s}_{mi} + \tilde{n}_{mi}, \tag{4.12}$$

where

$$\tilde{s}_{mi} = s_{mi}cos(\phi_{mi}) + js_{mi}sin(\phi_{mi}), \tag{4.13}$$

$$\tilde{n}_{mi} = n_{mic} + jn_{mis} \tag{4.14}$$

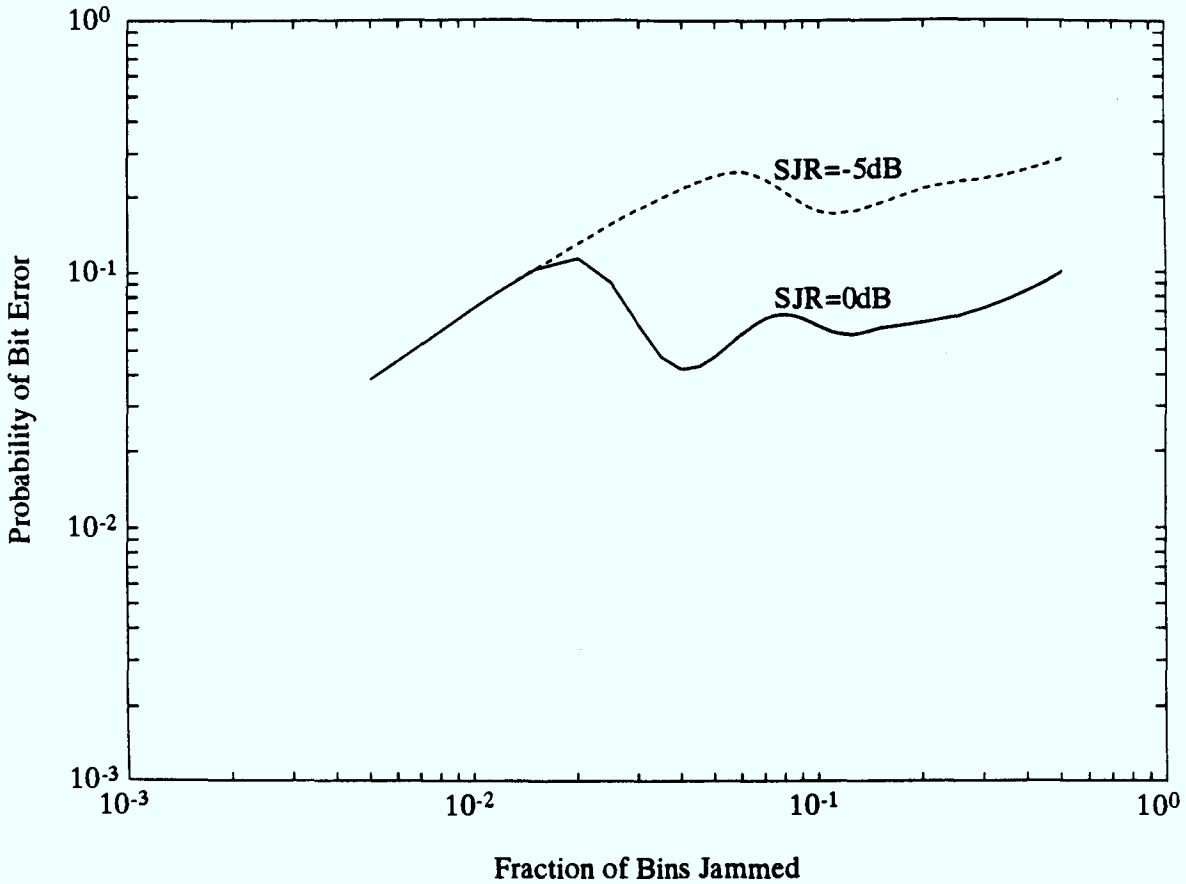

Figure 4.3: P_b for Houston-sense multiple-tone jamming, $L = 8$, $M = 2$, $SNR = 10$ dB.

The noise components, n_{mic} and n_{mis}, are Gaussian random variables with zero mean and variance,

$$\sigma_n^2 = \frac{N_0}{2T_h} \tag{4.15}$$

where $N_0/2$ is the double-sided power spectral density of the noise, and T_h is the hop period. The signal amplitude, s_{mi}, is a random variable with pdf,

$$f_{s_{mi}}(s_{mi}) = \frac{s_{mi}}{s_0^2} \exp(-\frac{s_{mi}^2}{2s_0^2}), s_{mi} \geq 0. \tag{4.16}$$

For $s_{mi} < 0$, $f_{s_{mi}}(s_{mi}) = 0$. The mean power of the signal is $2s_0^2$. From 3.10, the two-dimensional characteristic function of the matched filter output sample is

$$\Phi_{\tilde{y}_{mi}}(\rho) = \exp(-\frac{\rho^2(\sigma_n^2 + s_0^2)}{2}). \tag{4.17}$$

The pdf of the output sample with signal and noise present is

$$f_{sn}(z_{mi}) = \frac{z_{mi}}{\sigma_T^2} \exp(\frac{-z_{mi}^2}{2\sigma_T^2}), z_{mi} \geq 0, \tag{4.18}$$

where $\sigma_T^2 = \sigma_n^2 + s_0^2$. For $z_{mi} < 0$, $f_{sn}(z_{mi}) = 0$. The pdf of the output sample with only noise present is

$$f_n(z_{mi}) = \frac{z_{mi}}{\sigma_n^2} \exp(\frac{-z_{mi}^2}{2\sigma_n^2}), z_{mi} \geq 0. \tag{4.19}$$

For $z_{mi} < 0$, $f_n(z_{mi}) = 0$.

4.4.2 The 2-1- and 4-2-Moment Method

In the 2-1-moment method, a decision statistic, v_m, is formed by (2.22). For $L = 2$, the decision statistic is after simplification

$$v_m = z_{m1} z_{m2}. \tag{4.20}$$

Define a variable $q = z_{m2}$. The joint pdf of v_m and q is found from the joint pdf of z_{m1} and z_{m2}. Because of the independence of z_{m1} and z_{m2}, the joint pdf of z_{m1} and z_{m2} is the product of the individual pdf. Thus, the joint pdf is

$$f_{z_{m1},z_{m2}}(z_{m1}, z_{m2}) = \frac{z_{m1} z_{m2}}{\sigma^4} \exp(\frac{-z_{m1}^2 - z_{m2}^2}{2\sigma^2}), z_{m1} \geq 0, z_{m2} \geq 0. \tag{4.21}$$

The magnitude of the jacobian of the transformation from (z_{m1}, z_{m2}) to (v_m, q) is

$$|J(z_{m1}, z_{m2})| = q. \tag{4.22}$$

The joint pdf of v_m and q is [53]

$$f_{v_m,q}(v_m,q) = \frac{f_{z_{m1},z_{m2}}(z_{m1},z_{m2})}{|J(z_{m1},z_{m2})|} \tag{4.23}$$

where $z_{m1} = v_m/q$ and $z_{m2} = q$. Thus, substituting (4.21) and (4.22) into (4.23),

$$f_{v_m,q}(v_m,q) = \frac{v_m}{q\sigma^4}\exp(\frac{-(\frac{v_m}{q})^2 - q^2}{2\sigma^2}), v_m \geq 0, q \geq 0. \tag{4.24}$$

The pdf of v_m can be found by integrating (4.24) with respect to q. Thus,

$$f_{v_m}(v_m) = \int_0^\infty \frac{v_m}{q\sigma^4}\exp(\frac{-\frac{v_m{}^2}{q} - q^2}{2\sigma^2})dq, v_m \geq 0. \tag{4.25}$$

Simplifying [54],

$$f_{v_m}(v_m) = \frac{v_m}{\sigma^4}K_0(\frac{v_m}{\sigma^2}), v_m \geq 0, \tag{4.26}$$

where $K_0()$ is the zeroth-order modified-Bessel function. By integrating (4.26), the cdf of v_m can be found as

$$F_{v_m}(v_m) = \int_0^{v_m} f_{v_m}(x)dx, v_m \geq 0. \tag{4.27}$$

Simplifying [3],

$$F_{v_m}(v_m) = 1 - \frac{v_m}{\sigma^2}K_1(\frac{v_m}{\sigma^2}), v_m \geq 0, \tag{4.28}$$

where $K_1()$ is the first-order modified-Bessel function.

The bit-error probability, P_b, for binary NCFSK can be found by

$$\begin{aligned} P_b &= 1 - \int_0^\infty F_n(v)f_{sn}(v)dv && (4.29)\\ &= \int_0^\infty \frac{v^2}{\sigma_n^4\sigma_T^2}K_0(\frac{v}{\sigma_T^2})K_1(\frac{v}{\sigma_n^2})dv && (4.30)\\ &= (\frac{\sigma_n}{\sigma_T})^4{}_2F_1(2,1;3;1-(\frac{\sigma_n}{\sigma_T})^4) && (4.31)\\ &= (\frac{\sigma_n}{\sigma_T})^4\sum_{k=0}^\infty \frac{1}{k+2}(1-(\frac{\sigma_n}{\sigma_T})^4)^k && (4.32)\\ &= \frac{(\frac{\sigma_n}{\sigma_T})^4}{(1-(\frac{\sigma_n}{\sigma_T})^4)^2}(4\ln(\frac{\sigma_T}{\sigma_n}) + (\frac{\sigma_n}{\sigma_T})^4 - 1) && (4.33) \end{aligned}$$

where $F_n()$ is the cdf of v_m with only noise present, $f_{sn}()$ is the pdf of v_m with signal plus noise present, and ${}_2F_1(,;;)$ is the Gauss hypergeometric function. The expression for P_b in (4.33) is a new result. The 4-2-moment method has identical performance to that of the 2-1-moment method for $L = 2$ and $M = 2$ in independent Rayleigh fading.

4.4.3 Linear Diversity Combining

For linear diversity combining, a decision statistic, v_m, is formed by (2.9). For $L = 2$, the cdf of v_m can be computed as

$$F_{v_m}(v_m) = \int_0^{v_m} \int_0^{v_m - z_{m1}} \frac{z_{m1} z_{m2}}{\sigma^4} \exp(\frac{-z_{m1}^2 - z_{m2}^2}{2\sigma^2}) dz_{m1} dz_{m2}. \tag{4.34}$$

Simplifying,

$$F_{v_m}(v_m) = 1 - \exp(\frac{-v_m^2}{2\sigma^2}) - \frac{v_m\sqrt{2}}{2\sigma} \exp(\frac{-v_m^2}{4\sigma^2}) \text{erf}(\frac{v_m}{2\sigma}), v_m \geq 0, \tag{4.35}$$

where

$$\text{erf}(z) = \frac{2}{\sqrt{\pi}} \int_0^z \exp(-t^2) dt, v_m \geq 0. \tag{4.36}$$

The pdf of v_m can be found by differentiating (4.35). Thus,

$$f_{v_m}(v_m) = \frac{v_m}{2\sigma} \exp(\frac{-v_m^2}{2\sigma^2}) - \frac{\sqrt{\pi}}{4\sigma^3}(v_m^2 + 2\sigma^2) \exp(\frac{-v_m^2}{4\sigma^2}) \text{erf}(\frac{v_m}{2\sigma}), v_m \geq 0. \tag{4.37}$$

The probability of bit error for binary NCFSK must be found numerically by integrating

$$P_b = 1 - \int_0^\infty F_n(v) f_{sn}(v) dv. \tag{4.38}$$

4.4.4 Square-Law Diversity Combining

For square-law diversity combining, a decision statistic, v_m, is formed as (2.11). For $L = 2$, the pdf and cdf are given by [55]

$$f_{v_m}(v_m) = \frac{v_m}{4\sigma^4} \exp(-\frac{v_m}{2\sigma^2}), v_m \geq 0, \tag{4.39}$$

and

$$F_{v_m}(v_m) = 1 - (1 + \frac{v_m}{2\sigma^2}) \exp(-\frac{v_m}{2\sigma^2}), v_m \geq 0, \tag{4.40}$$

After considerable algebraic manipulation, the probability of bit error is given by

$$P_b = \frac{4 + 3\beta}{8 + 12\beta + 6\beta^2 + \beta^3} = \frac{4 + 3\beta}{(2 + \beta)^3} \tag{4.41}$$

where $\beta = SNR = s_0^2/\sigma_n^2$. This result agrees with [5].

4.4.5 Results

The bit-error probability was computed for $L = 2$ and $M = 2$ in independent Rayleigh fading using (4.38), (3.27), and (3.28) for linear combining, using (4.33) for the 4-2- and

2-1-moment-method combining, and using (4.41) for square-law combining. The results are shown in Fig. 4.4. Square-law combining has the best performance. The 4-2- and 2-1-moment-method combining have the second best performance. Linear combining has the worst performance. However, linear combining is only 1.9 dB worse than square-law combining. Square-law combining can be shown to be the optimum combining method in independent Rayleigh fading.

4.5 Summary

This chapter presented performance results for the demodulation of FFH NCFSK systems with time diversity and linear diversity combining. These results were obtained using a novel analytical technique described in the previous chapter.

In broad-band noise, for linear combining, the probability of bit error decreases as the level of diversity is increased. Also in broad-band noise, linear and square-law combining have similar performance. In multiple-tone jamming, Houston-sense jamming is not necessarily the worst-case jamming. In Rayleigh fading with $M = 2$ and $L = 2$, square-law combining performs better than the 4-2-moment-method, 2-1-moment-method and linear combining.

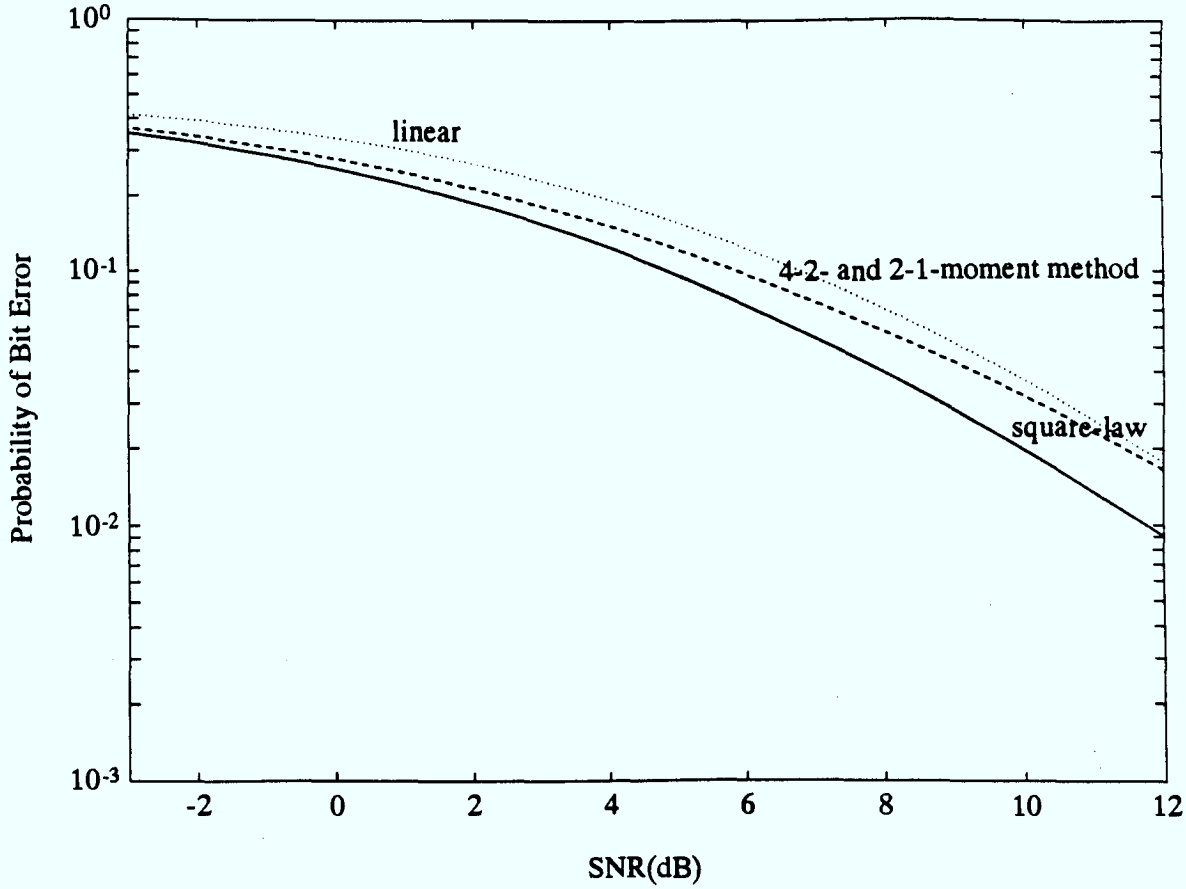

Figure 4.4: P_b with $M = 2$ and $L = 2$ in independent Rayleigh fading.

Chapter 5

Application to Uplink Coarse-Time Synchronization for a FFH NCFSK Satellite-Communication System

5.1 Introduction

The analysis method of Chapter 3 is applied to uplink coarse-time synchronization of a FFH NCFSK satellite-communication system with time diversity and linear diversity combining. The decision statistics, v_p and v_e for $e = 1, ..., E$, are formed from the matched-filter output samples, z_{pi} and z_{ei} for $i = 1, ..., L$, and $e = 1, ..., E$, by linear combining. The probe-bin statistic, v_p, is compared to a threshold, v_t. There are numerous methods of obtaining a value for the threshold, v_t. For illustration, the "adaptive-threshold method" is used. For comparison, the ideal value of v_t based upon perfect knowledge of σ is used.

In the adaptive-threshold method, a new value of v_t is obtained for every new v_p and is based upon the sum, v_e, obtained in a single empty bin ($E = 1$). The means of obtaining the value of v_t is based on the following observations and assumptions. Suppose that the interference in the empty bin were only WGN of two-sided power-spectral density, $N_0/2$. Then, [52]

$$E[v_e] = L\sqrt{\frac{\pi}{2}}\sigma \tag{5.1}$$

where $\sigma^2 = N_0/2T_h$. Thus, an estimate of σ is

$$\hat{\sigma} = \frac{v_e}{L}\sqrt{\frac{2}{\pi}}. \tag{5.2}$$

It can be shown that for a particular value of the probability of false alarm, the threshold is $v_t = c_a\sigma$ where c_a is a constant that is independent of σ. The constant, c_a, is computed separately once. Then, each new threshold can be calculated from the estimate, $\hat{\sigma}$, given via (5.2) by

$$v_t = \frac{c_a}{L}\sqrt{\frac{2}{\pi}}v_e = b_a v_e \tag{5.3}$$

where $b_a = (c_a/L)\sqrt{2/\pi}$ is a constant. A similar method for setting the threshold is described in [56]. Clearly, if the interference is not Gaussian, the threshold will be set improperly, and the probability of false alarm will differ from its expected value.

For the ideal value of v_t, the actual (not estimated) value of σ for WGN is used to obtain $E[v_e]$ according to (5.1). The threshold is set to $v_t = b_f E[v_e]$ where b_f is a constant chosen to give the desired false-alarm probability.

The probability of synchronization-probe-burst detection was computed for two different types of jamming: (1) broad-band noise, and (2) multiple-tone jamming plus broad-band noise. It is assumed in the calculations that the synchronization-probe burst is either perfectly aligned, i.e. $\Delta T = 0$, or else $|\Delta T| > T_h$. This means that there is no spillover from the probe bin to the empty bin. The analysis can be easily modified for $|\Delta T| \neq 0$, or $|\Delta T| < T_h$.

5.2 Broad-Band Noise

For the adaptive-threshold method, the probability of detection in broad-band noise is given by

$$P_d = \int_0^{LR} (1 - F_{v_p}(b_a v_e)) f_{v_e}(v_e) dv_e, \tag{5.4}$$

and the probability of detection with an ideal threshold in broad-band noise is given by

$$P_d = 1 - F_{v_p}(b_f E[v_e]) \tag{5.5}$$

where the required cdf and pdf are calculated from (3.15),(3.16),(3.27), and (3.28) with the subscript, m, replaced by p or e. The signal is a constant tone with rms amplitude, s_{pi}, and the noise is AWGN. The signal-to-noise ratio after dehopping is given by (4.1).

The constants are set so that $P_{fa} = 0.01$. The probability of false alarm can be computed using (5.4) and (5.5) with $F_{v_e}()$ substituted for $F_{v_p}()$ and P_{fa} substituted for P_d.

Various constants are tried until $P_{fa} = 0.01$ The constants are set as follows: $b_f = 2.4215$ for $L = 1$ and an ideal threshold, $b_a = 1.8744$ for $L = 8$, $E = 1$ and an adaptive threshold, and $b_f = 1.4584$ for $L = 8$ and an ideal threshold. The adaptive-Romberg method was used for the numerical integration [47] with $\delta = 10^{-8}$. To calculate the Fourier-Bessel series of (3.15) and (3.16), 150 terms were used. To calculate the Fourier series of (3.27) and (3.28), 40 nonzero terms were used. With the above choices, the results have an accuracy of $\pm 10^{-8}$.

Fig. 5.1 shows the performance in broad-band noise. Three curves are shown: $L = 1$ and an ideal threshold, $L = 8$ and an ideal threshold, and $L = 8$, $E = 1$, and an adaptive threshold. The performance with $L = 8$, $E = 1$ and an adaptive threshold is about 2.7 dB better than the performance without diversity and an ideal threshold. However, the method with $L = 8$ requires eight times as many probes as the method without any diversity. The performance with $L = 8$ and an ideal threshold is a further 3.2 dB better than the performance with $L = 8$, $E = 1$ and an adaptive threshold. The ideal-threshold method represents the performance with a perfect threshold-setting algorithm. It is unattainable in practice, but provides a bound on achievable performance. If more empty bins are used to set the threshold, this bound can be approached. For example, if eight empty bins were used ($E = 8$), the performance of the adaptive threshold method was calculated and found to be within a fraction of a dB of that with an ideal threshold.

5.3 Multiple-Tone Jamming

The probability of detection was computed in this section for multiple-tone jamming plus broad-band noise. Jammer tones are randomly located in a fraction, γ, of the total number of bins and are assumed to have the same amplitude, $a_{pi} = a_{ei}$. Each tone's center is at the center of the corresponding frequency bin. Out of L hops, the probe bin would contain a signal tone and noise every time, but would contain a jammer tone l_p times where l_p is a random integer with $0 \leq l_p \leq L$. Similarly, out of L hops, the empty bin would contain noise every time, but would contain a jammer tone l_e times where l_e is a random integer with $0 \leq l_e \leq L$. The probability of each combination of tone jamming is calculated from (4.7). The probability of detection for each combination of tone jamming, $P_d(l_e, l_p)$, is calculated using (5.4) with $P_d(l_e, l_p)$ substituted for P_d where the required cdf and pdf are calculated by (3.15) and (3.16) with the appropriate characteristic functions used. The probability of false alarm for each combination of tone jamming, $P_{fa}(l_e, l_p)$, is

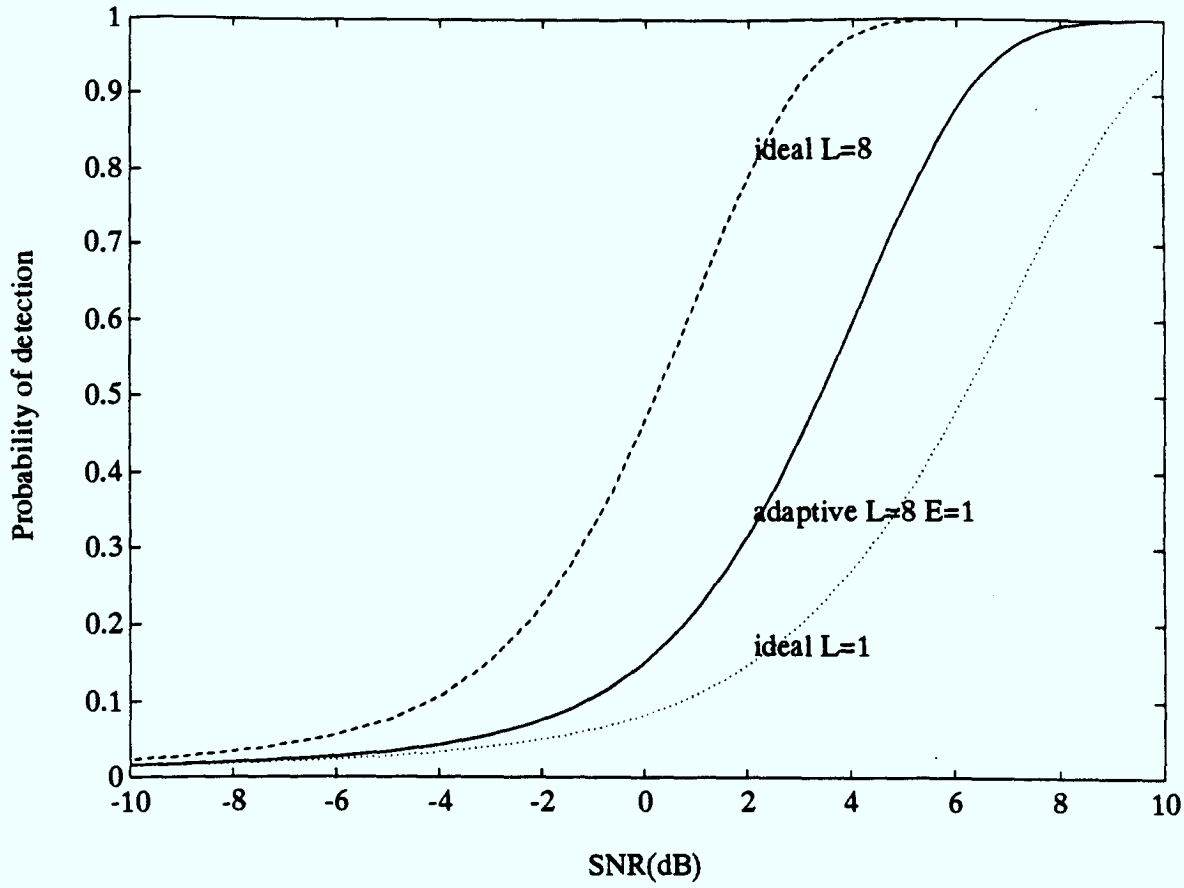

Figure 5.1: The probability of detection in broad-band noise ($P_{fa} = 0.01$).

calculated using (5.4) with $P_{fa}(l_e, l_p)$ substituted for P_d and $F_{v_e}()$ substituted for $F_{v_p}()$ where the required cdf and pdf are calculated by (3.15) and (3.16) with the appropriate characteristic functions used. The probability of probe-burst detection is given by

$$P_d = \sum_{l_e=0}^{L} \sum_{l_p=0}^{L} P_{comb}(l_e, l_p) P_d(l_e, l_p). \tag{5.6}$$

The probability of probe-burst false alarm is given by

$$P_{fa} = \sum_{l_e=0}^{L} \sum_{l_p=0}^{L} P_{comb}(l_e, l_p) P_{fa}(l_e, l_p). \tag{5.7}$$

The signal-to-noise ratio is given by (4.1). The ratio of signal to tone jammer is given by (4.6). The constant was set equal to $b_a = 1.8744$ so that the P_{fa} would be 0.01 in broad-band noise. The adaptive-Romberg method was used for the numerical integration [47] with $\delta = 10^{-6}$. To calculate the Fourier-Bessel series of (3.15) and (3.16), 150 terms were used. To calculate the Fourier series of (3.27) and (3.28), 200 nonzero terms were used. With the above choices, the results have an accuracy of $\pm 10^{-6}$. Fig. 5.2 and Fig. 5.3 show the performance of with $L = 8$, $E = 1$, and an adaptive threshold in broad-band noise and multiple-tone jamming.

In Fig. 5.2, $SNR = 10$ dB and $SJR = 0$ dB. The probability of detection is at a maximum for a jamming fraction of $\gamma = 0.0$ and at a minimum for broad-band jamming ($\gamma = 1.0$). The probability of false alarm has a maximum at $\gamma \approx 0.08$ and a minimum at $\gamma = 0.0$ and $\gamma = 1.0$. For broad-band noise jamming of the same total power ($SNR = -0.4$ dB), the probability of detection is $P_d \approx 0.16$, and the probability of false alarm is $P_{fa} = 0.01$.

In Fig. 5.3, $SNR = 10$ dB and $SJR = 5$ dB. The probability of detection is also at a maximum for a jamming fraction of $\gamma = 0.0$ and at a minimum for broad-band jamming ($\gamma = 1.0$). The probability of false alarm has a maximum at $\gamma \approx 0.04$ and a minimum at $\gamma = 0.0$ and $\gamma = 1.0$. The curve in Fig. 5.3 is not monotonically decreasing as is the one in Fig. 5.2. For broad-band noise jamming of the same total power ($SNR = 3.8$ dB), the probability of detection is $P_d \approx 0.57$, and the probability of false alarm is $P_{fa} = 0.01$.

Note that the lowest probability of detection is achieved with broad-band jamming ($\gamma = 1.0$). Thus, jamming only a fraction of the total number of bins is not effective in reducing the probability of detection. However, the probability of false alarm has a maximum at some intermediate value of jamming fraction ($0.0 < \gamma < 1.0$). Hence, jamming only a fraction of the total number of bins can be used to increase the false-alarm probability. Also, the probability of detection and probability of false alarm are

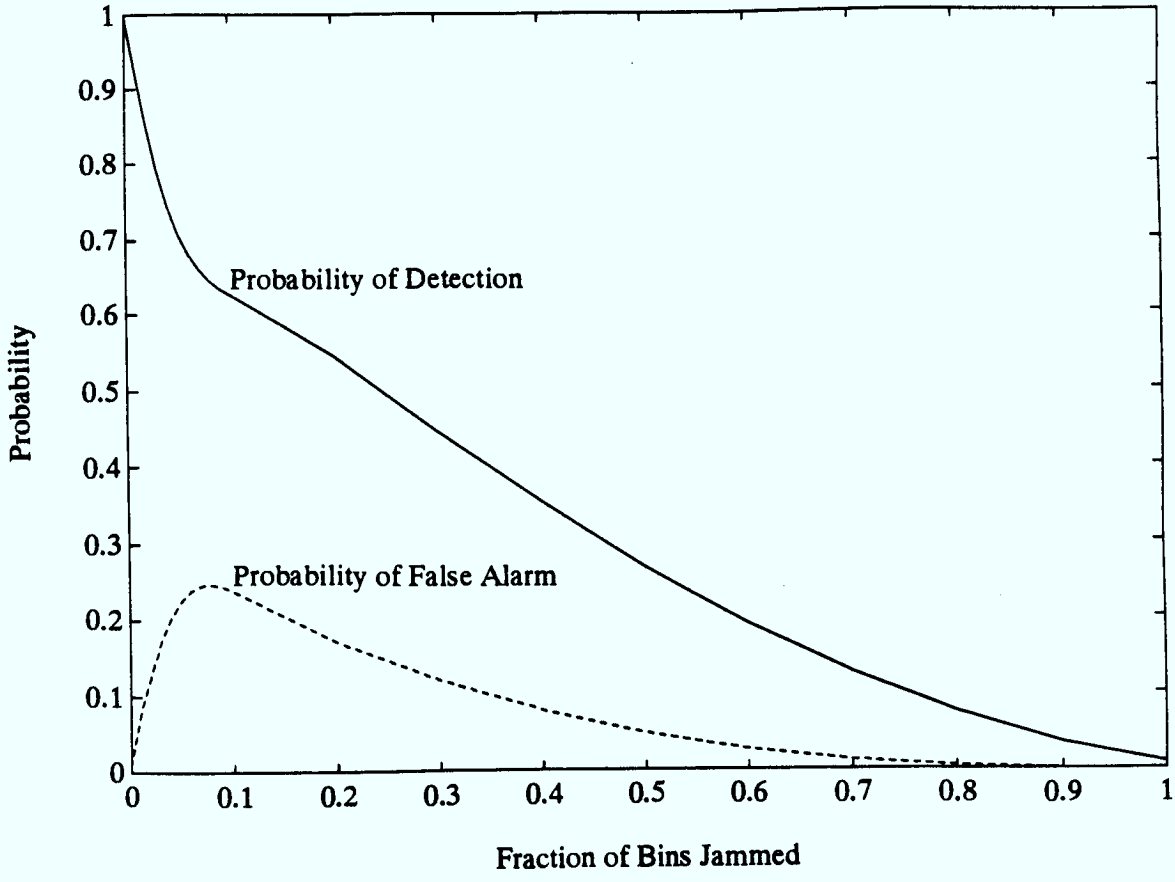

Figure 5.2: Noise and tone jamming performance for adaptive-threshold method, $L = 8$, $SNR = 10$ dB, $SJR = 0$ dB.

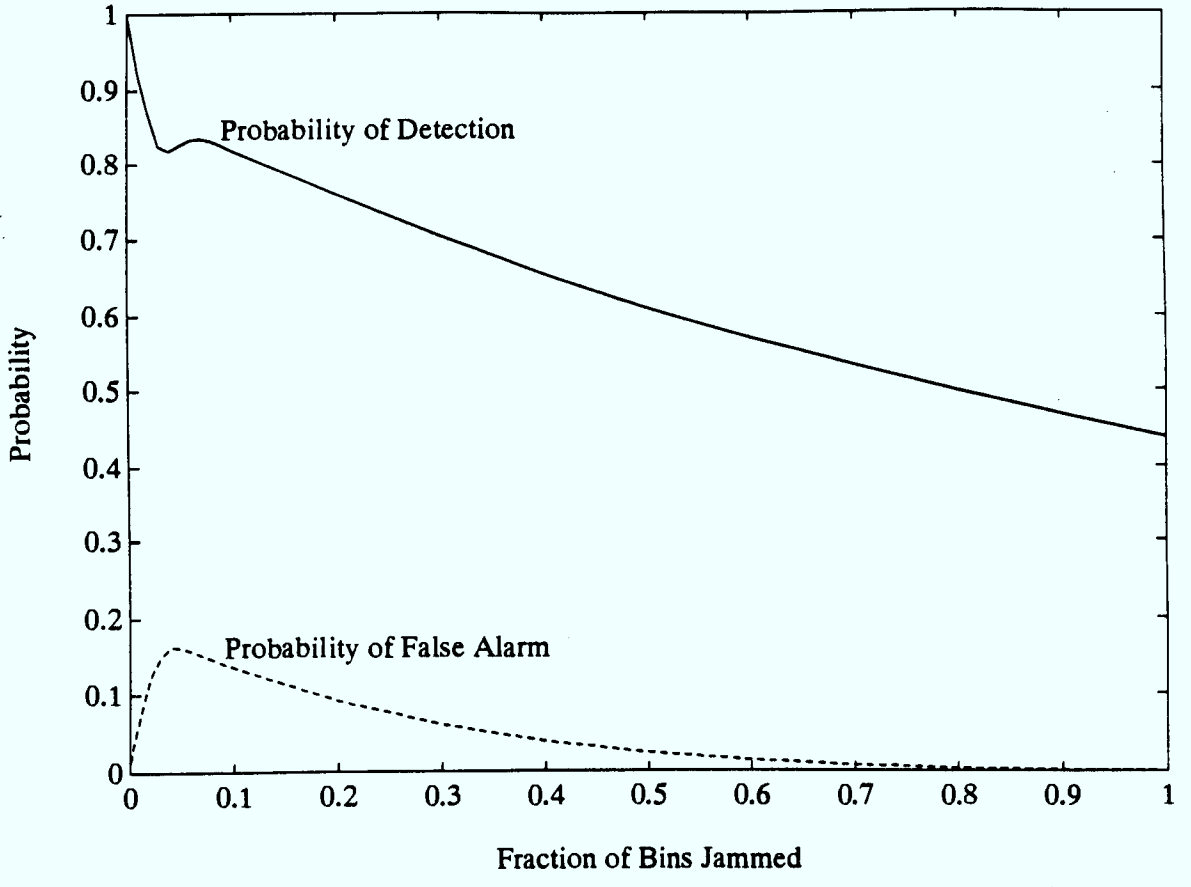

Figure 5.3: Noise and tone jamming performance for adaptive-threshold method, $L = 8$, $SNR = 10$ dB, $SJR = 5$ dB.

both lower for broad-band tone jamming with broad-band noise jamming than for only broad-band noise jamming.

5.4 Summary

This chapter presents the performance of an uplink-coarse-time-synchronization algorithm for a FFH NCFSK satellite-communication system with time diversity and linear diversity combining in noise jamming and multiple-tone jamming. Results show that time diversity and linear diversity combining can be used to improve performance in broad-band noise. Results also show that the adaptive-threshold method does not have a constant false-alarm probability for multiple-tone jamming. With multiple-tone jamming, the minimum probability of detection is achieved by jamming the entire band; however, the maximum probability of false alarm is achieved by jamming only part of the entire band.

Chapter 6

Conclusions

6.1 Summary

This report has provided a literature review of diversity-combining techniques and analysis methods as applied to these techniques. References have been provided for the use of these techniques in demodulation, coarse-time synchronization and fine-time synchronization.

An analytical method has been developed for one of the techniques, linear combining. The method combines circularly symmetric function theory, Fourier-Bessel series, and Fourier series. With this method, the bit-error probability for demodulation and the probability of detection for coarse-time synchronization have been computed. Where possible, the results obtained with this method were compared to other reported results, and the two results agreed well. Also, several new results were also obtained.

Linear combining was shown to be a near-optimal scheme in broad-band noise. Its performance is similar to that of square-law combining in broad-band noise. In multiple-tone jamming, the worst-case jamming depends on signal-to-noise ratio for linear combining. For high signal-to-noise ratios, the worst-case is Houston-sense jamming with a relatively small jamming fraction. Randomly distributed jamming with a relatively small jamming fraction is almost as bad. However, for low signal-to-noise ratios, the worst-case is jamming every bin.

A novel analytical result was derived for the 4-2- and 2-1-moment methods in independent Rayleigh fading. An expression is obtained for the probability of bit error with $L = 2$ and $M = 2$. For this situation, linear combining is a little bit worse than square-law combining, 2-1-moment-method combining, and 4-2-moment-method combining. However,

other situations should be examined before conclusions can be drawn.

Other diversity-combining methods are very difficult to analyze. The difficulty often arises because the decision statistics are correlated. Perhaps, further research will find ways around this problem.

6.2 Recommendations

Linear combining is an excellent method in broad-band noise. In severe multiple-tone jamming, linear combining is good. In weak multiple-tone jamming, linear combining is not a good method because it is susceptible to Houston-sense multiple-tone jamming with a small jamming fraction. In independent Rayleigh fading, square-law combining is the best method for the particular situation that was considered.

6.3 Future Work

Future work should include: accuracy considerations for the analytical method, ways to improve accuracy of the analytical method, other diversity-combining techniques, extension of fading work, acquisition-time computation for coarse-time synchronization, analysis of fine-time synchronization, and experimental verification of results.

Bibliography

[1] H.L. Van Trees, *Detection, Estimation and Modulation Theory*, part 1, New York:Wiley, 1968.

[2] C.J. Waylan, "Detection of fast, noncoherent, frequency-hopped FSK," *IEEE Trans. Commun.*, vol. COM-23, pp. 543-546, May 1975.

[3] M. Abramowitz and I.A. Stegun, *Handbook of Mathematical Functions*, New York:Dover, 1964.

[4] R.A. Yost, "On the Symbiotic Nature of Key Antijamming and Antiscintillation Functions for MFSK and DPSK Channels," *IEEE J. Select. Areas Commun.*, vol. SAC-8, pp. 887-894, June 1990.

[5] J.N. Pierce, "Theoretical diversity improvement in frequency-shift keying," *Proc. IRE*, vol. 46, pp. 903-910, May 1958.

[6] B.K. Levitt, "Use of diversity to improve FH/MFSK performance in worst case partial band noise and multitone jamming," in *Proc. IEEE Milcom*, 1982, pp. 28.2.1-28.2.5.

[7] C.M. Keller and M.B. Pursley, "Clipped diversity combining for channels with partial-band interference - part I: clipped-linear combining," *IEEE Trans. Commun.*, vol. COM-35, pp. 1320-1328, Dec. 1987.

[8] S.L. March and J.A. Ritcey, "Performance of an order statistic based diversity combining M-ary frequency-hopping system in a partial-band jamming environment," in *Proc. IEEE Milcom*, 1989, pp. 11-15.

[9] E.B. Felstead and T.A. Gulliver, "Improving the ECCM performance of fast frequency hopping by diversity combining," in *Proc. AGARD Symp. ECCM Avion. Sens. Commun. Syst.*, 1990, pp. 28.1-28.10.

[10] P.M. Hahn, "Theoretical diversity improvement in multiple frequency shift keying," *Proc. IRE*, vol. 50, pp. 177-184, June 1962.

[11] W.C. Lindsey, "Error probability for Rician fading multichannel reception of binary and N-ary signals," *IEEE Trans. Inform. Theory*, vol. IT-10, pp. 339-350, Oct. 1964.

[12] W.C. Lindsey, "Error probability for incoherent diversity reception," *IEEE Trans. Inform. Theory*, vol. IT-11, pp. 491-499, Oct. 1965.

[13] K.S. Gong, "Performance of diversity combining techniques for FH/MFSK in worst case partial band noise and multi-tone jamming," in *Proc. IEEE Milcom*, 1983, pp. 17-21.

[14] J.S. Lee, R.H. French and L.E. Miller, "Probability of error analyses of a BFSK frequency-hopping system with diversity under partial-band jamming interference - part I: performance of square-law linear combining soft decision receiver," *IEEE Trans. Commun.*, vol. COM-32, pp. 645-653, June 1984.

[15] J.S. Bird and E.B. Felstead, "Antijam performance of fast frequency-hopped M-ary NCFSK - an overview," *IEEE J. Select. Areas Commun.*, vol. SAC-4, pp. 216-233, Mar. 1986.

[16] P. Tardiff and E.B. Felstead, "Measurement of diversity-combining performance enhancement for fast-FH," in *Proc. IEEE Milcom*, 1989, paper 16-19.

[17] C.M. Keller and M.B. Pursley, "Clipped diversity combining for channels with partial-band interference - part II: ratio-statistic combining," *IEEE Trans. Commun.*, vol. COM-37, pp. 145-151, Feb. 1989.

[18] Y.T. Su, "Fast FH/MFSK communications in band multitone jamming: performance of a class of self-normalizing receivers," in *Proc. IEEE Milcom*, 1988, pp 809-813.

[19] T.A. Gulliver and E.B. Felstead, "Moment methods for diversity combining of fast frequency hopped noncoherent MFSK," in *Proc. Queen's 15th Bi. Symp. Commun.*, 1990, pp. 13-16.

[20] T.A. Gulliver, "Diversity combining and Reed-Solomon coding for fast frequency hopped noncoherent MFSK," in *Proc. IEEE Milcom*, 1990, pp. 106-110.

[21] R.C. Robertson and T.T. Ha, "Error probabilities of frequency-hopped FSK with self-normalization combining in a fading channel with partial-band interference," in *Proc. IEEE Milcom*, 1990, pp. 511-515.

[22] L.E. Miller, J.S. Lee and A.P. Kadrichu, "Probability of error analyses of a BFSK frequency-hopping system with diversity under partial-band jamming interference - part III: performance of square-law self-normalizing soft decision receiver," *IEEE Trans. Commun.*, vol. COM-34, pp. 669-675, July 1986.

[23] C.M. Keller and M.B. Pursley, "Diversity combining for channels with fading and partial-band interference," *IEEE J. Select. Areas Commun.*, vol. SAC-5, pp. 248-260, Feb. 1987.

[24] G. Li, Q. Wang, V.K. Bhargava and L.J. Mason, "Performance analysis of a ratio-threshold diversity combining scheme in FFH/FSK spread spectrum systems under multitone jamming," in *Proc. IEEE Milcom*, 1991, pp. 1240-1244.

[25] J.A. Ritcey, "Performance analysis of a robust BFSK FH-SS communication system in partial-band noise jamming," in *Proc. IEEE Milcom*, 1986, pp. 2.7.1-2.7.5.

[26] T.A. Gulliver, "Order statistics diversity combining in worst-case noise and multitone jamming," in *Proc. IEEE Milcom*, 1991, pp. 385-389.

[27] T.A. Gulliver, "New diversity combining techniques for improving the performance of fast frequency hopping," in *Proc. Int. Conf. Adv. Commun. Control Syst.*, 1991.

[28] M.K. Simon, J.K. Omura, R.A. Scholtz and B.K. Levitt, *Spread Spectrum Communications*, vol. 3, Rockville:Computer Science Press, 1985.

[29] L. Biederman, "Uplink coarse acquisition for a mobile user satellite system," in *Proc. ICC*, 1982, pp. 6H.6.1-6H.6.5.

[30] M.A. Blanco, "A self-probing method for time synchronization of frequency-hopped spread spectrum signals," in *Proc. IEEE Milcom*, 1984, pp. 110-114.

[31] S.J. Simmons and P. Lamers, "Coarse synchronization in an EHF frequency-hopped satellite communication system," in *Proc. CCECE*, 1990, pp. 36.1.1-36.1.4.

[32] T.A. Gulliver, "A moment method for the detection of synchronization probes in worst case noise and multitone jamming," in *Proc. IEEE Milcom*, 1991, pp 1054-1058.

[33] R. Ezers, E.B. Felstead, T.A. Gulliver and J.S. Wight, "A method for the analysis of diversity combining for the detection of FH synchronization probes," in *Proc. IEEE Milcom*, 1991, pp. 591-595.

[34] D.M. Hodsdon, "A satellite FSK demodulator, using an analog SAW chirp Fourier transformer," in *Proc. AIAA Twelfth Int. Commun. Sat. Sys. Conf.*, 1988, pp. 561-568.

[35] L.J. Mason and E.B. Felstead, "Consistent estimation methods for the fine-time synchronization of FH systems," in *Proc. IEEE Milcom*, 1989, pp. 895-899.

[36] D.G. Brennan, "Linear diversity combining techniques," *Proc. IRE*, vol. 47, pp. 1075-1102, June 1959.

[37] J.I. Marcum, "A statistical theory of target detection by pulsed radar," *IRE Trans. Inform. Theory*, vol. IT-6, pp. 269-308, April 1960.

[38] N.C. Beaulieu, "An infinite series for the computation of the complementary probability distribution function of a sum of independent random variables and its application to the sum of Rayleigh random variables," *IEEE Trans. Commun.*, vol. COM-38, pp. 1463-1474, Sept. 1990.

[39] C.W. Helstrom, "Performance of receivers with linear detectors," *IEEE Trans. Aerosp. Electron. Syst.*, vol. AES-26, pp. 210-217, Mar. 1990.

[40] J.S. Bird and D.A. George, "The use of Fourier-Bessel series in calculating the error probabilities for digital communication systems," *IEEE Trans. Commun.*, vol. COM-29, pp. 1357-1365, Sept. 1981.

[41] J.S. Bird, "Calculating detection probabilities for systems employing noncoherent integration," *IEEE Trans. Aerosp. Electron. Syst.*, vol. AES-18, pp. 401-409, July 1982.

[42] R. Esposito and L.R. Wilson, "Statistical properties of two sine waves in Gaussian noise," *IEEE Trans. Inform. Theory*, vol. IT-19, pp. 176-183, Mar. 1973.

[43] J. Goldman, "Statistical properties of a sum of sinusoids and Gaussian noise and its generalization to higher dimensions," *Bell Syst. Tech. J.*, vol. 53, pp. 557-580, Apr. 1974.

[44] R. Price, "An orthonormal Laguerre expansion yielding Rice's envelope density function for two sine waves in noise," *IEEE Trans. Inform. Theory*, vol. IT-34, pp. 1375-1382, Nov. 1988.

[45] S.O. Rice, "Probability distributions of noise plus several sine waves - the problem of computation," *IEEE Trans. Commun.*, vol. COM-22, pp. 851-853, June 1974.

[46] C.W. Helstrom, "Distribution of the sum of two sine waves and Gaussian noise," *IEEE Trans. Inform. Theory*, vol. IT-38, pp. 186-191, Jan. 1992.

[47] W.H. Press, B.P. Flannery, S.A. Teukolsky, and W.T. Vetterling, *Numerical Recipes in C*, New York:Cambridge, 1988.

[48] H. Bateman, *Higher Transcendental Functions*, New York:McGraw-Hill, 1953.

[49] R. Barakat, "First-order statistics of combined random sinusoidal waves with applications to laser speckle patterns," *Opt. Acta*, vol. 21, no. 11, pp. 903-921, 1974.

[50] J.K. Jao and M. Elbaum, "First-order statistics of a non-Rayleigh fading signal and its detection," *Proc. IEEE*, vol. 66, pp. 781-789, July 1978.

[51] S.W. Houston, "Modulation techniques for communication, part 1: tone and noise jamming performance of spread spectrum M-ary FSK and 2, 4-ary DPSK waveforms," in *Proc. IEEE NAECON*, 1975, pp. 51-58.

[52] T.R. Benedict and T.T. Soong, "The joint estimation of signal and noise from the sum envelope," *IEEE Trans. Inform. Theory*, vol. IT-13, pp. 447-454, July 1967.

[53] A. Papoulis, *Probability, Random Variables, and Stochastic Processes*, McGraw-Hill: New York, 1984.

[54] I.S. Gradshteyn and I.M. Ryzhik, *Table of Integrals, Series, and Products*, Academic:San Diego, 1980.

[55] J.G. Proakis, *Digital Communications*, McGraw-Hill:New York, 1983.

[56] J.S. Bird, "Calculating detection probabilities for adaptive thresholds," *IEEE Trans. Aerosp. Electron. Syst.*, vol. AES-19, pp. 506-512, July 1983.

DOCUMENT CONTROL DATA

(Security classification of title, body of abstract and indexing annotation must be entered when the overall document is classified)

1. ORIGINATOR (the name and address of the organization preparing the document. Organizations for whom the document was prepared, e.g. Establishment sponsoring a contractor's report, or tasking agency, are entered in section 8.)

Carleton University, Department of Electronics, Ottawa, Ontario, K1S 5B6

2. SECURITY CLASSIFICATION (overall security classification of the document including special warning terms if applicable)

UNCLASSIFIED

3. TITLE (the complete document title as indicated on the title page. Its classification should be indicated by the appropriate abbreviation (S,C,R or U) in parentheses after the title.)

Analysis of Time-Diversity Combining Methods for Frequency-Hopped Signals (U)

4. AUTHORS (Last name, first name, middle initial. If military, show rank, e.g. Doe, Maj. John E.)

Ezers, Rolands E., and Wight, James S.

5. DATE OF PUBLICATION (month and year of publication of document)

April 1992

6a. NO. OF PAGES (total containing information. Include Annexes, Appendices, etc.)

61

6b. NO. OF REFS (total cited in document)

56

7. DESCRIPTIVE NOTES (the category of the document, e.g. technical report, technical note or memorandum. If appropriate, enter the type of report, e.g. interim, progress, summary, annual or final. Give the inclusive dates when a specific reporting period is covered.)

Final Report

8. SPONSORING ACTIVITY (the name of the department project office or laboratory sponsoring the research and development. Include the address.)

Defence Research Establishment Ottawa, Ottawa, Ontario, K1A 0Z4

9a. PROJECT OR GRANT NO. (if appropriate, the applicable research and development project or grant number under which the document was written. Please specify whether project or grant)

Project Number 041LL-A3

9b. CONTRACT NO. (if appropriate, the applicable number under which the document was written)

36001-1-3515

10a. ORIGINATOR'S DOCUMENT NUMBER (the official document number by which the document is identified by the originating activity. This number must be unique to this document.)

DOE-92-09

10b. OTHER DOCUMENT NOS. (Any other numbers which may be assigned this document either by the originator or by the sponsor)

11. DOCUMENT AVAILABILITY (any limitations on further dissemination of the document, other than those imposed by security classification)

(X) Unlimited distribution
( ) Distribution limited to defence departments and defence contractors; further distribution only as approved
( ) Distribution limited to defence departments and Canadian defence contractors; further distribution only as approved
( ) Distribution limited to government departments and agencies; further distribution only as approved
( ) Distribution limited to defence departments; further distribution only as approved
( ) Other (please specify):

12. DOCUMENT ANNOUNCEMENT (any limitation to the bibliographic announcement of this document. This will normally correspond to the Document Availability (11). However, where further distribution (beyond the audience specified in 11) is possible, a wider announcement audience may be selected.)

Unlimited

13. ABSTRACT (a brief and factual summary of the document. It may also appear elsewhere in the body of the document itself. It is highly desirable that the abstract of classified documents be unclassified. Each paragraph of the abstract shall begin with an indication of the security classification of the information in the paragraph (unless the document itself is unclassified) represented as (S), (C), (R), or (U). It is not necessary to include here abstracts in both official languages unless the text is bilingual).

Fast-frequency-hopped (FFH) noncoherent-frequency-shift-keyed (NCFSK) systems with time diversity and diversity combining are discussed in this report. A literature review of diversity-combining techniques is provided. An analytical method has been developed for one of the techniques, linear combining. The method combines circularly symmetric function theory, Fourier-Bessel series, and Fourier series. With this method, the bit-error probability for the demodulation of FFH NCFSK systems with time diversity and linear diversity combining and the probability of detection and probability of false alarm for uplink coarse-time synchronization of a FFH NCFSK satellite-communication system with time diversity and linear diversity combining have been computed in broad-band noise and multiple-tone jamming. Where possible, the results obtained with this method were compared to other reported results, and the two results agreed well. A novel analytical result was derived for computing the bit-error probability for the demodulation of FFH NCFSK systems with time diversity and 4-2- or 2-1-moment-method diversity combining in independent Rayleigh fading.

For demodulation, linear diversity combining is an excellent method in broad-band noise. In severe multiple-tone jamming, linear diversity combining is good. In weak multiple-tone jamming, linear diversity combining is not a good method because it is susceptible to Houston-sense multiple-tone jamming with a small jamming fraction. In independent Rayleigh fading, square-law combining is the best method for the particular situation which was considered.

For uplink coarse-time synchronization, time diversity and linear diversity combining could be used to improve performance.

14. KEYWORDS, DESCRIPTORS or IDENTIFIERS (technically meaningful terms or short phrases that characterize a document and could be helpful in cataloguing the document. They should be selected so that no security classification is required. Identifiers, such as equipment model designation, trade name, military project code name, geographic location may also be included. If possible, keywords should be selected from a published thesaurus, e.g. Thesaurus of Engineering and Scientific Terms (TEST) and that thesaurus identified. If it is not possible to select indexing terms which are Unclassified, the classification of each should be indicated as with the title.)

- Frequency hopping
- Spread-spectrum communications
- Satellite communications
- Diversity combining
- Time diversity
- Linear combining
- M-ary NCFSK modulation
- Coarse-time synchronization
- Multiple-tone jamming
- Noise jamming

DATE DUE

MAY 20 1997			
JUN 24 1997			
AOUT 8 1997			

[redacted]